Quantifying the performance of approximate teleportation and quantum error correction via symmetric 2-PPT-extendible channels

Tharon Holdsworth [1,2], Vishal Singh [2,3] and Mark M. Wilde [2,4]

[1]*Department of Physics, University of Alabama at Birmingham, Birmingham, Alabama 35233, USA*
[2]*Hearne Institute for Theoretical Physics, Department of Physics and Astronomy, and Center for Computation and Technology, Louisiana State University, Baton Rouge, Louisiana 70803, USA*
[3]*School of Applied and Engineering Physics, Cornell University, Ithaca, New York 14850, USA*
[4]*School of Electrical and Computer Engineering, Cornell University, Ithaca, New York 14850, USA*

(Received 9 August 2022; accepted 7 December 2022; published 26 January 2023)

The ideal realization of quantum teleportation relies on having access to a maximally entangled state; however, in practice, such an ideal state is typically not available and one can instead only realize an approximate teleportation. With this in mind, we present a method to quantify the performance of approximate teleportation when using an arbitrary resource state. More specifically, after framing the task of approximate teleportation as an optimization of a simulation error over one-way local operations and classical communication (LOCC) channels, we establish a semidefinite relaxation of this optimization task by instead optimizing over the larger set of 2-PPT-extendible channels (where PPT denotes positive partial transpose). The main analytical calculations in our paper consist of exploiting the unitary covariance symmetry of the identity channel to establish a significant reduction of the computational cost of this latter optimization. Next, by exploiting known connections between approximate teleportation and quantum error correction, we also apply these concepts to establish bounds on the performance of approximate quantum error correction over a given quantum channel. Finally, we evaluate our bounds for various examples of resource states and channels.

DOI: 10.1103/PhysRevA.107.012428

I. INTRODUCTION

Teleportation is one of the most basic protocols in quantum information science [1]. By means of two bits of classical communication and an entangled pair of qubits (a so-called resource state), it is possible to transmit a qubit from one location to another. This protocol demonstrates the fascinating possibilities available under the distant laboratories paradigm of local operations and classical communication (LOCC), and it prompted the development of the resource theory of entanglement [2]. Teleportation is so ubiquitous in quantum information science now, that nearly every subfield (fault-tolerant computing, error correction, cryptography, communication complexity, Shannon theory, etc.) employs it in some manner. A number of impressive teleportation experiments have been conducted over the past few decades [3–10].

The teleportation protocol assumes an ideal resource state; however, if the resource state shared between the two parties is imperfect, then the teleportation protocol no longer simulates an ideal quantum channel, but rather some approximation of it [11,12]. This problem has been studied considerably in the literature and is related to the well-known problem of entanglement distillation [2,13]. Recently, it has been addressed in a precise and general operational way, in terms of a meaningful channel distinguishability measure [14, Definition 19].

In the seminal work [2], a connection was forged between entanglement distillation and approximate quantum error correction. There it was shown that certain one-way LOCC entanglement distillation protocols can be converted to approximate quantum error correction protocols, and vice versa. Thus, techniques for analyzing entanglement distillation can be used to analyze quantum error correction and vice versa.

In this paper, we obtain bounds on the performance of teleportation when using an imperfect resource state, and by exploiting the aforementioned connection, we address a related problem for approximate quantum error correction. We thus consider our paper to offer two distinct, yet related contributions. The conceptual approach that we take here is linked to that of [15], which was concerned with a more involved protocol called bidirectional teleportation; it is also linked to [16,17], which introduced the set of k-extendible channels as a semidefinite relaxation of the set of one-way LOCC channels. Our approach has strong links as well with that taken in [18], the latter concerned with bounding the performance of approximate quantum error correction by means of k-PPT-extendible channels; these channels were introduced in [18] as a semidefinite relaxation of the set of one-way LOCC channels that forms a tighter containment than k-extendible channels alone. In fact, our method applied to the problem of approximate quantum error correction can be understood as exploiting further symmetries available when simulating the identity channel, in order to reduce the computational complexity required to calculate the bounds given in [18].

Let us discuss our first contribution in a bit more detail. Suppose that the goal is to use a bipartite resource state ρ_{AB}

along with one-way LOCC to simulate a perfect quantum channel of dimension d. It is not always possible to perform this simulation exactly, and for most resource states, an error will occur. We can quantify the simulation error either in terms of the diamond distance [19] or the channel infidelity [20]. However, we prove here that the simulation error is the same, regardless of whether we use the channel infidelity or the diamond distance, when quantifying the deviation between the simulation and an ideal quantum channel (note that a similar result was found previously in [15] and we exploit similar techniques to arrive at our conclusion here). Next, in order to obtain a lower bound on the simulation error, and due to the fact that it is computationally challenging to optimize over one-way LOCC channels, we optimize the error over the larger set of 2-PPT-extendible channels (where PPT denotes positive partial transpose; defined in Sec. II B 5) and show that the resulting quantity can be calculated by means of a semidefinite program. By exploiting the unitary covariance symmetry of the ideal quantum channel, we reduce the computational complexity of the semidefinite program to depend only on the dimension of the resource state ρ_{AB} being considered. This constitutes our main contribution to the analysis of teleportation with an imperfect resource state. We also provide a general formulation of the simulation problem when trying to simulate an arbitrary channel using one-way LOCC and a resource state.

The second contribution of our paper employs a similar line of reasoning to obtain a lower bound on the simulation error of approximate quantum error correction. In this setting, instead of a bipartite state, two parties have at their disposal a quantum channel $\mathcal{N}_{A\to B}$, for which they can prepend an encoding and append a decoding in order to simulate a perfect quantum channel of dimension d. This encoding and decoding can be understood as a superchannel [21] that transforms $\mathcal{N}_{A\to B}$ into an approximation of the perfect quantum channel. It is clear that the simulation error cannot increase by allowing for a superchannel realized by one-way local operations and common randomness (LOCR), and here, following the approach outlined above, we find a lower bound on the simulation error by optimizing instead over the larger class of 2-PPT-extendible superchannels with an extra nonsignaling constraint. Critically, this lower bound can be calculated by means of a semidefinite program. As indicated above, this problem was previously considered in [18], but our contribution is that the semidefinite programming lower bound reported here has a substantially reduced computational complexity, depending only on the input and output dimensions of the channel $\mathcal{N}_{A\to B}$ of interest.

A. Organization of the paper

Our paper is organized into two major parts, according to the contributions mentioned above. The first part (Secs. II–IV) details our contribution to quantifying the performance of approximate teleportation. The second part (Secs. V–VII) details our contribution to quantifying the performance of approximate quantum error correction.

The first part of our paper is organized as follows: Sec. II provides some background on quantum states and channels, with an emphasis on LOCC and LOCR bipartite channels. Section III establishes a measure for the performance of quantum channel simulation, namely, in terms of the normalized diamond distance and channel infidelity. We prove here that these two error measures are equal when the goal is to simulate the identity channel, following as a consequence of the unitary covariance symmetry of the identity channel. Section IV presents the major contribution of the first part, a semidefinite program (SDP) that gives a lower bound on the simulation error of approximate teleportation when using an arbitrary bipartite resource state and one-way LOCC channels. This SDP is further simplified by exploiting the aforementioned symmetry of the identity channel to reduce the computational cost of the optimization task significantly.

The second part of our paper is organized as follows: Sec. V provides background on quantum superchannels to generalize the concepts of one-way LOCC and LOCR bipartite channels to superchannels. Section VI explores the task of channel simulation, i.e., simulating a quantum channel from an arbitrary quantum channel and LOCR superchannels. The performance of channel simulation is again quantified with the normalized diamond distance and channel infidelity, and again the error measures are equal when the goal is to simulate the identity channel with the assistance of common randomness. Section VII presents the major contribution of the second part, an SDP that gives a lower bound on the error in simulating a quantum channel with an arbitrary channel and LOCR superchannels. We detail a much simplified SDP for the simulation of an identity channel, the case of interest in approximate quantum error correction, by leveraging its unitary covariance symmetry.

Section VIII presents plots that result from numerical calculations of our SDP error bounds. The first example in Sec. VIII A bounds the error in approximate teleportation using a certain mixed state as the resource state, demonstrating that 2-PPT-extendiblity constraints can achieve tighter bounds when compared to PPT constraints alone. The second example in Sec. VIII B considers the bounds when using a lower dimensional resource state to simulate a higher dimensional identity channel. The next example in Sec. VIII C considers the bounds for qubit and qutrit depolarizing channels. The penultimate example in Sec. VIII D bounds the error in approximate teleportation when using two-mode squeezed states as the resource state. The final example in Section VIII E bounds the error in simulating an identity channel when using the three-level amplitude damping channel [22], and it is thus an example of our bound applied to approximate quantum error correction.

Section IX concludes by discussing several open questions for future work. We note here that Python code for calculating the SDPs in our paper is available with its arXiv posting.

II. BACKGROUND ON STATES, CHANNELS, AND BIPARTITE CHANNELS

We recall some basic facts about quantum information theory in this section to fix our notation before proceeding; more detailed background can be found in [23–27].

A. States and channels

A quantum state or density operator, usually denoted by ρ_A, σ_A, etc., is a positive semidefinite, unit trace operator acting on a Hilbert space $\mathcal{H}_A$. The Heisenberg-Weyl operators are unitary transformations of quantum states, defined for all $x, z \in \{0, 1, \ldots, d-1\}$ as

$$Z(z) := \sum_{k=0}^{d-1} e^{\frac{2\pi i k z}{d}} |k\rangle\langle k|, \tag{1}$$

$$X(x) := \sum_{k=0}^{d-1} |k \oplus_d x\rangle\langle k|, \tag{2}$$

$$W^{z,x} := Z(z)X(x), \tag{3}$$

where $\oplus_d$ denotes addition modulo d.

A quantum channel is a completely positive (CP), trace-preserving (TP) map. Let $\mathcal{N}_{A\to B}$ denote a quantum channel that accepts as input a linear operator acting on a Hilbert space $\mathcal{H}_A$ and outputs a linear operator acting on a Hilbert space $\mathcal{H}_B$. For short, we say that the channel takes system A to system B, where systems are identified with Hilbert spaces. Let $\Gamma^{\mathcal{N}}_{RB}$ denote the Choi operator of a channel $\mathcal{N}_{A\to B}$:

$$\Gamma^{\mathcal{N}}_{RB} := \mathcal{N}_{A\to B}(\Gamma_{RA}), \tag{4}$$

where

$$\Gamma_{RA} := \sum_{i,j=0}^{d_A-1} |i\rangle\langle j|_R \otimes |i\rangle\langle j|_A \tag{5}$$

is the unnormalized maximally entangled operator and $\{|i\rangle_R\}_{i=0}^{d_A-1}$ and $\{|i\rangle_A\}_{i=0}^{d_A-1}$ are orthonormal bases.

The Choi representation of a channel is isomorphic to the superoperator representation and provides a convenient means of characterizing a channel. Namely, a channel $\mathcal{M}_{A\to B}$ is completely positive if and only if its Choi operator $\Gamma^{\mathcal{M}}_{RB}$ is positive semidefinite and a channel $\mathcal{M}_{A\to B}$ is trace preserving if and only if its Choi operator $\Gamma^{\mathcal{M}}_{RB}$ satisfies $\mathrm{Tr}_B[\Gamma^{\mathcal{M}}_{RB}] = I_R$.

B. Bipartite channels

A bipartite channel $\mathcal{N}_{AB\to A'B'}$ maps input systems A and B to output systems A' and B'. In this model, we assume that a single party Alice has access to systems A and A', while another party Bob has access to systems B and B'. The Choi operator for a bipartite channel $\mathcal{N}_{AB\to A'B'}$ is as follows:

$$\Gamma^{\mathcal{N}}_{\tilde{A}\tilde{B}A'B'} = \mathcal{N}_{AB\to A'B'}(\Gamma_{\tilde{A}A} \otimes \Gamma_{\tilde{B}B}). \tag{6}$$

1. One-way LOCC channels

A bipartite channel $\mathcal{L}_{AB\to A'B'}$ is a one-way LOCC (1WL) channel if it can be written as follows:

$$\mathcal{L}_{AB\to A'B'} = \sum_x \mathcal{E}^x_{A\to A'} \otimes \mathcal{D}^x_{B\to B'}, \tag{7}$$

where $\{\mathcal{E}^x_{A\to A'}\}_x$ is a set of completely positive maps, such that the sum map $\sum_x \mathcal{E}^x_{A\to A'}$ is trace preserving, and $\{\mathcal{D}^x_{B\to B'}\}_x$ is a set of quantum channels. The idea here is that Alice acts on her system A with a quantum instrument described by $\{\mathcal{E}^x_{A\to A'}\}_x$, transmits the classical outcome x of the measurement over a classical communication channel to Bob, who subsequently applies the quantum channel $\mathcal{D}^x_{B\to B'}$ to his system B. A key example of a one-way LOCC channel is in the teleportation protocol: given that Alice and Bob share a maximally entangled state in systems $\hat{A}\hat{B}$ and Alice has prepared the system A_0 that she would like to teleport, the one-way LOCC channel consists of Alice performing a Bell measurement on systems $A_0\hat{A}$ (quantum instrument), sending the measurement outcome to Bob (classical communication), who then applies a Heisenberg-Weyl correction operation on system B conditioned on the classical communication from Alice. One-way LOCC channels are central in our analysis of approximate teleportation.

2. LOCR channels

A subset of one-way LOCC channels consists of those that can be implemented by local operations and common randomness (LOCR). These channels have the following form:

$$\mathcal{C}_{AB\to A'B'} = \sum_y p(y)\mathcal{E}^y_{A\to A'} \otimes \mathcal{D}^y_{B\to B'}, \tag{8}$$

where $\{p(y)\}_y$ is a probability distribution and $\{\mathcal{E}^y_{A\to A'}\}_y$ and $\{\mathcal{D}^y_{B\to B'}\}_y$ are sets of quantum channels. The main difference between one-way LOCC and LOCR is that, in the latter case, the channel is simply a probabilistic mixture of local channels. In order to simulate them, classical communication is not needed, and only the weaker resource of common randomness is required. Thus, the following containment holds:

$$\mathrm{LOCR} \subset \mathrm{1WL}. \tag{9}$$

These channels play a role in our analysis of approximate quantum error correction and channel simulation.

3. 2-extendible channels

A bipartite channel $\mathcal{N}_{AB\to A'B'}$ is 2-extendible [16,17], if there exists an extension channel $\mathcal{M}_{AB_1B_2\to A'B'_1B'_2}$ satisfying permutation covariance:

$$\mathcal{M}_{AB_1B_2\to A'B'_1B'_2} \circ \mathcal{F}_{B_1B_2} = \mathcal{F}_{B'_1B'_2} \circ \mathcal{M}_{AB_1B_2\to A'B'_1B'_2} \tag{10}$$

and the following nonsignaling constraint:

$$\mathrm{Tr}_{B_2'} \circ \mathcal{M}_{AB_1B_2\to A'B'_1B'_2} = \mathcal{N}_{AB_1\to A'B'_1} \otimes \mathrm{Tr}_{B_2}. \tag{11}$$

In the above, $\mathcal{F}_{B_1B_2}$ is the unitary swap channel that permutes systems B_1 and B_2, and $\mathcal{F}_{B'_1B'_2}$ is defined similarly. Also, Tr denotes the partial trace channel. Note that the two conditions in (10) and (11) imply that the original channel $\mathcal{N}_{AB\to A'B'}$ is nonsignaling from Bob to Alice,

$$\mathrm{Tr}_{B'} \circ \mathcal{N}_{AB\to A'B'} = \mathrm{Tr}_{B'} \circ \mathcal{N}_{AB\to A'B'} \circ \mathcal{R}^{\pi}_B, \tag{12}$$

where

$$\mathcal{R}^{\pi}_B(\cdot) := \mathrm{Tr}[\cdot]\pi_B \tag{13}$$

is a replacer channel that traces out its input and replaces it with the maximally mixed state $\pi_B := \frac{I}{d_B}$. We provide a proof of (12) in Appendix.

More generally, k-extendible channels were defined in [16,17], and a resource theory was constructed based on them. However, we only make use of 2-extendible channels in this work, and we leave the study of our problem using

k-extendible channels for future work. See [18] for an alternative definition of k-extendible channels that appeared after the original proposal of [16]. A key insight of [16,17] is that the set of one-way LOCC channels is contained in the set of 2-extendible channels, and we make use of this observation in our paper.

A bipartite channel $\mathcal{N}_{AB\to A'B'}$ is 2-extendible if and only if its Choi operator $\Gamma^{\mathcal{N}}_{ABA'B'}$ is such that there exists a Hermitian operator $\Gamma^{\mathcal{M}}_{AB_1B_2A'B_1'B_2'}$ satisfying [16,17]

$$\left(\mathcal{F}_{B_1B_2}\otimes\mathcal{F}_{B_1'B_2'}\right)\left(\Gamma^{\mathcal{M}}_{AB_1B_2A'B_1'B_2'}\right)=\Gamma^{\mathcal{M}}_{AB_1B_2A'B_1'B_2'}, \tag{14}$$

$$\operatorname{Tr}_{B_2'}\left[\Gamma^{\mathcal{M}}_{AB_1B_2A'B_1'B_2'}\right]=\Gamma^{\mathcal{N}}_{AB_1A'B_1'}\otimes I_{B_2}, \tag{15}$$

$$\Gamma^{\mathcal{M}}_{AB_1B_2A'B_1'B_2'}\geqslant 0, \tag{16}$$

$$\operatorname{Tr}_{A'B_1'B_2'}\left[\Gamma^{\mathcal{M}}_{AB_1B_2A'B_1'B_2'}\right]=I_{AB_1B_2}. \tag{17}$$

The condition in (14) holds if and only if (10) does. The condition in (15) holds if and only if (11) does. Finally, (16) holds if and only if $\mathcal{M}_{AB_1B_2\to A'B_1'B_2'}$ is completely positive, and (17) holds if and only if $\mathcal{M}_{AB_1B_2\to A'B_1'B_2'}$ is trace preserving. Related to the above, the conditions in (14) and (15) imply the following nonsignaling condition on the Choi operator of $\mathcal{N}_{AB\to A'B'}$:

$$\operatorname{Tr}_{B'}\left[\Gamma^{\mathcal{N}}_{ABA'B'}\right]=\frac{1}{d_B}\operatorname{Tr}_{BB'}\left[\Gamma^{\mathcal{N}}_{ABA'B'}\right]\otimes I_B, \tag{18}$$

which is equivalent to (12).

4. Completely positive-partial-transpose preserving channels

A bipartite channel $\mathcal{N}_{AB\to A'B'}$ is completely positive-partial-transpose preserving (C-PPT-P) [28,29] if the map $T_{B'}\circ\mathcal{N}_{AB\to A'B'}\circ T_B$ is completely positive. Here T_B is the partial transpose map, defined as the following superoperator:

$$T_B(\cdot)\coloneqq\sum_{i,j}|i\rangle\langle j|_B(\cdot)|i\rangle\langle j|_B. \tag{19}$$

See also [30]. The set of one-way LOCC channels is contained in the set of C-PPT-P channels [28,29], and we also make use of this observation in our paper. A bipartite channel $\mathcal{N}_{AB\to A'B'}$ is C-PPT-P if and only if its Choi operator $\Gamma^{\mathcal{N}}_{ABA'B'}$ satisfies

$$\Gamma^{\mathcal{N}}_{ABA'B'}\geqslant 0, \tag{20}$$

$$\operatorname{Tr}_{A'B'}\left[\Gamma^{\mathcal{N}}_{ABA'B'}\right]=I_{AB}, \tag{21}$$

$$T_{BB'}\left(\Gamma^{\mathcal{N}}_{ABA'B'}\right)\geqslant 0, \tag{22}$$

where $T_{BB'}$ is the partial transpose acting on systems B and B'. We note that the C-PPT-P constraint has been used in prior work on bounding the simulation error in bidirectional teleportation [15]. See also [31–35] for other contexts.

5. 2-PPT-extendible channels

We can combine the above constraints in a nontrivial way to define the set of 2-PPT-extendible channels, and we note that this was considered recently in [18, Remark after Lemma 4.10], as a generalization of the concept employed for bipartite states [36,37]. Explicitly, a bipartite channel $\mathcal{N}_{AB\to A'B'}$ is 2-PPT-extendible if there exists an extension channel $\mathcal{M}_{AB_1B_2\to A'B_1'B_2'}$ satisfying the following conditions of permutation covariance, nonsignaling, and being completely-PPT-preserving:

$$\mathcal{M}_{AB_1B_2\to A'B_1'B_2'}\circ\mathcal{F}_{B_1B_2}=\mathcal{F}_{B_1'B_2'}\circ\mathcal{M}_{AB_1B_2\to A'B_1'B_2'}, \tag{23}$$

$$\operatorname{Tr}_{B_2'}\circ\mathcal{M}_{AB_1B_2\to A'B_1'B_2'}=\mathcal{N}_{AB_1\to A'B_1'}\otimes\operatorname{Tr}_{B_2}, \tag{24}$$

$$T_{B_2'}\circ\mathcal{M}_{AB_1B_2\to A'B_1'B_2'}\circ T_{B_2}\in\mathrm{CP}, \tag{25}$$

$$T_{A'}\circ\mathcal{M}_{AB_1B_2\to A'B_1'B_2'}\circ T_A\in\mathrm{CP}. \tag{26}$$

It is redundant to demand further that the following constraints hold:

$$T_{B_1'}\circ\mathcal{M}_{AB_1B_2\to A'B_1'B_2'}\circ T_{B_1}\in\mathrm{CP}, \tag{27}$$

$$T_{A'B_1'}\circ\mathcal{M}_{AB_1B_2\to A'B_1'B_2'}\circ T_{AB_1}\in\mathrm{CP}, \tag{28}$$

$$T_{A'B_2'}\circ\mathcal{M}_{AB_1B_2\to A'B_1'B_2'}\circ T_{AB_2}\in\mathrm{CP}, \tag{29}$$

$$T_{B_1'B_2'}\circ\mathcal{M}_{AB_1B_2\to A'B_1'B_2'}\circ T_{B_1B_2}\in\mathrm{CP}, \tag{30}$$

because they follow as a consequence of (25) and (23), (25), (27), and (26), respectively. A bipartite channel $\mathcal{N}_{AB\to A'B'}$ is 2-PPT-extendible if and only if its Choi operator $\Gamma^{\mathcal{N}}_{ABA'B'}$ is such that there exists a Hermitian operator $\Gamma^{\mathcal{M}}_{AB_1B_2A'B_1'B_2'}$ satisfying

$$\left(\mathcal{F}_{B_1B_2}\otimes\mathcal{F}_{B_1'B_2'}\right)\left(\Gamma^{\mathcal{M}}_{AB_1B_2A'B_1'B_2'}\right)=\Gamma^{\mathcal{M}}_{AB_1B_2A'B_1'B_2'}, \tag{31}$$

$$\operatorname{Tr}_{B_2'}\left[\Gamma^{\mathcal{M}}_{AB_1B_2A'B_1'B_2'}\right]=\Gamma^{\mathcal{N}}_{AB_1A'B_1'}\otimes I_{B_2}, \tag{32}$$

$$T_{B_2B_2'}\left(\Gamma^{\mathcal{M}}_{AB_1B_2A'B_1'B_2'}\right)\geqslant 0, \tag{33}$$

$$T_{AA'}\left(\Gamma^{\mathcal{M}}_{AB_1B_2A'B_1'B_2'}\right)\geqslant 0, \tag{34}$$

$$\Gamma^{\mathcal{M}}_{AB_1B_2A'B_1'B_2'}\geqslant 0, \tag{35}$$

$$\operatorname{Tr}_{A'B_1'B_2'}\left[\Gamma^{\mathcal{M}}_{AB_1B_2A'B_1'B_2'}\right]=I_{AB_1B_2}. \tag{36}$$

Observe that a bipartite channel $\mathcal{N}_{AB\to A'B'}$ is C-PPT-P if it is 2-PPT-extendible. This follows from (24) and (26).

Every one-way LOCC channel of the form in (7) is 2-PPT-extendible by considering the following extension channel:

$$\sum_x\mathcal{E}^x_{A\to A'}\otimes\mathcal{D}^x_{B_1\to B_1'}\otimes\mathcal{D}^x_{B_2\to B_2'}, \tag{37}$$

which manifestly satisfies the constraints in (23)–(26). We thus employ 2-PPT-extendible channels as a semidefinite relaxation of the set of one-way LOCC channels.

6. 2-PPT-extendible nonsignaling channels

We can add a further constraint to the channels discussed in the previous section, i.e., a nonsignaling constraint of the following form:

$$\operatorname{Tr}_{A'}\circ\mathcal{M}_{AB_1B_2\to A'B_1'B_2'}=\operatorname{Tr}_{A'}\circ\mathcal{M}_{AB_1B_2\to A'B_1'B_2'}\circ\mathcal{R}^{\pi}_A, \tag{38}$$

which ensures that the extension channel $\mathcal{M}_{AB_1B_2\to A'B_1'B_2'}$ is also nonsignaling from Alice to both Bobs. The constraint on the Choi operator $\Gamma^{\mathcal{M}}_{AB_1B_2A'B_1'B_2'}$ is as follows:

$$\operatorname{Tr}_{A'}\left[\Gamma^{\mathcal{M}}_{AB_1B_2A'B_1'B_2'}\right]=\frac{1}{d_A}\operatorname{Tr}_{A'A}\left[\Gamma^{\mathcal{M}}_{AB_1B_2A'B_1'B_2'}\right]\otimes I_A. \tag{39}$$

Every LOCR channel of the form in (8) is 2-PPT-extendible nonsignaling, as is evident by choosing the

following extension channel:

$$\sum_y p(y)\mathcal{E}^y_{A\to A'}\otimes\mathcal{D}^y_{B_1\to B_1'}\otimes\mathcal{D}^y_{B_2\to B_2'}. \tag{40}$$

We thus employ 2-PPT-extendible nonsignaling channels as a semidefinite relaxation of the set of LOCR channels, and we note here that [18] previously used this approach.

Let us state explicitly here that extensions of one-way LOCC channels of the form in (7) generally do not satisfy the nonsignaling constraint in (38), due to the fact that each map $\mathcal{E}^x_{A\to A'}$ in (7) is not necessarily trace preserving.

III. QUANTIFYING THE PERFORMANCE OF APPROXIMATE TELEPORTATION

In approximate teleportation, Alice and Bob are allowed to make use of a fixed bipartite state $\rho_{\hat{A}\hat{B}}$ and an arbitrary one-way LOCC channel $\mathcal{L}_{A\hat{A}\hat{B}\to B}$, with the goal of simulating an identity channel of dimension d. To be clear, the one-way LOCC channel $\mathcal{L}_{A\hat{A}\hat{B}\to B}$ has the following form:

$$\mathcal{L}_{A\hat{A}\hat{B}\to B}(\omega_{A\hat{A}\hat{B}})=\sum_x\mathcal{D}^x_{\hat{B}\to B}(\mathrm{Tr}_{A\hat{A}}[\Lambda^x_{A\hat{A}}\omega_{A\hat{A}\hat{B}}]), \tag{41}$$

where $\{\Lambda^x_{A\hat{A}}\}_x$ is a positive operator-valued measure (satisfying $\Lambda^x_{A\hat{A}}\geqslant 0$ for all x and $\sum_x\Lambda^x_{A\hat{A}}=I_{A\hat{A}}$) and $\{\mathcal{D}^x_{\hat{B}\to B}\}_x$ is a set of quantum channels. We assume that the dimension of the systems $\hat{A}\hat{B}$ is finite, and we write the dimension of $\hat{A}$ as $d_{\hat{A}}$ and the dimension of $\hat{B}$ as $d_{\hat{B}}$. The approximate teleportation protocol realizes the following simulation channel $\widetilde{\mathcal{S}}_{A\to B}$ [12, Eq. (11)]:

$$\widetilde{\mathcal{S}}_{A\to B}(\omega_A):=\mathcal{L}_{A\hat{A}\hat{B}\to B}(\omega_A\otimes\rho_{\hat{A}\hat{B}}). \tag{42}$$

In the following subsections, we discuss two seemingly different ways of quantifying the simulation error.

A. Quantifying simulation error with normalized diamond distance

The standard metric for quantifying the distance between quantum channels is the normalized diamond distance [19]. See the related paper [15] for discussions of the operational significance of the diamond distance (see also [27]). For channels $\mathcal{N}_{C\to D}$ and $\widetilde{\mathcal{N}}_{C\to D}$, the diamond distance is defined as

$$\|\mathcal{N}_{C\to D}-\widetilde{\mathcal{N}}_{C\to D}\|_\diamond:=\sup_{\rho_{RC}}\|\mathcal{N}_{C\to D}(\rho_{RC})-\widetilde{\mathcal{N}}_{C\to D}(\rho_{RC})\|_1, \tag{43}$$

where the optimization is over every bipartite state ρ_{RC} with the reference system R arbitrarily large. The following equality is well known (see, e.g., [27]):

$$\|\mathcal{N}_{C\to D}-\widetilde{\mathcal{N}}_{C\to D}\|_\diamond=\sup_{\psi_{RC}}\|\mathcal{N}_{C\to D}(\psi_{RC})-\widetilde{\mathcal{N}}_{C\to D}(\psi_{RC})\|_1, \tag{44}$$

where the optimization is over every pure bipartite state ψ_{RC} with the reference system R isomorphic to the channel input system C. The normalized diamond distance is then given by

$$\tfrac{1}{2}\|\mathcal{N}_{C\to D}-\widetilde{\mathcal{N}}_{C\to D}\|_\diamond, \tag{45}$$

so that the resulting error takes a value between zero and one. The reduction in (44) implies that it is a computationally tractable problem to calculate the diamond distance, and in fact, one can do so by means of the following semidefinite program [38]:

$$\inf_{\lambda,Z_{RD}\geqslant 0}\left\{\begin{array}{l}\lambda:\lambda I_R\geqslant\mathrm{Tr}_D[Z_{RD}],\\ Z_{RD}\geqslant\Gamma^{\mathcal{N}}_{RD}-\Gamma^{\widetilde{\mathcal{N}}}_{RD}\end{array}\right\}, \tag{46}$$

where $\Gamma^{\mathcal{N}}_{RD}$ and $\Gamma^{\widetilde{\mathcal{N}}}_{RD}$ are the Choi operators of $\mathcal{N}_{C\to D}$ and $\widetilde{\mathcal{N}}_{C\to D}$, respectively.

The simulation error when using a bipartite state $\rho_{\hat{A}\hat{B}}$ and a one-way LOCC channel to simulate an identity channel $\mathrm{id}^d_{A\to B}$ of dimension d is given by

$$e_{1\mathrm{WL}}(\rho_{\hat{A}\hat{B}},\mathcal{L}_{A\hat{A}\hat{B}\to B}):=\tfrac{1}{2}\left\|\mathrm{id}^d_{A\to B}-\widetilde{\mathcal{S}}_{A\to B}\right\|_\diamond, \tag{47}$$

where the simulation channel $\widetilde{\mathcal{S}}_{A\to B}$ is defined in (42). Employing (44), we find that

$$e_{1\mathrm{WL}}(\rho_{\hat{A}\hat{B}},\mathcal{L}_{A\hat{A}\hat{B}\to B})=\sup_{\psi_{RA}}\tfrac{1}{2}\|\psi_{RA}-\mathcal{L}_{A\hat{A}\hat{B}\to B}(\psi_{RA}\otimes\rho_{\hat{A}\hat{B}})\|_1, \tag{48}$$

with ψ_{RA} a pure bipartite state such that system R is isomorphic to system A. We are interested in the minimum possible simulation error, and so we define

$$e_{1\mathrm{WL}}(\rho_{\hat{A}\hat{B}}):=\inf_{\mathcal{L}\in 1\mathrm{WL}}e_{1\mathrm{WL}}(\rho_{\hat{A}\hat{B}},\mathcal{L}_{A\hat{A}\hat{B}\to B}), \tag{49}$$

where we recall that 1WL denotes the set of one-way LOCC channels. The error $e_{1\mathrm{WL}}(\rho_{\hat{A}\hat{B}})$ is one kind of simulation error on which we are interested in obtaining computationally efficient lower bounds. Indeed, it is a computationally difficult problem to calculate $e_{1\mathrm{WL}}(\rho_{\hat{A}\hat{B}})$ directly, and so we instead resort to calculating lower bounds.

B. Quantifying simulation error with channel infidelity

Another measure of the simulation error is by means of the channel infidelity. Let us recall that the fidelity of states ω and τ is defined as [39]

$$F(\omega,\tau):=\|\sqrt{\omega}\sqrt{\tau}\|_1^2, \tag{50}$$

where $\|X\|_1:=\mathrm{Tr}[\sqrt{X^\dagger X}]$. From this measure, we can define a channel fidelity measure for channels $\mathcal{N}_{C\to D}$ and $\widetilde{\mathcal{N}}_{C\to D}$ as follows:

$$F(\mathcal{N},\widetilde{\mathcal{N}}):=\inf_{\rho_{RC}}F[\mathcal{N}_{C\to D}(\rho_{RC}),\widetilde{\mathcal{N}}_{C\to D}(\rho_{RC})], \tag{51}$$

where the optimization is over every bipartite state ρ_{RC} with the reference system R arbitrarily large. Similar to the diamond distance, it suffices to optimize the channel fidelity over every pure bipartite state ψ_{RC} with reference system R isomorphic to the channel input system C (see, e.g., [27]):

$$F(\mathcal{N},\widetilde{\mathcal{N}}):=\inf_{\psi_{RC}}F[\mathcal{N}_{C\to D}(\psi_{RC}),\widetilde{\mathcal{N}}_{C\to D}(\psi_{RC})]. \tag{52}$$

The square root of the channel fidelity can be calculated by means of the following semidefinite program [40,41]:

$$\sqrt{F}(\mathcal{N},\widetilde{\mathcal{N}})=\sup_{\lambda\geqslant 0,Q_{RD}}\lambda \tag{53}$$

subject to

$$\lambda I_R \leqslant \mathrm{Re}[\mathrm{Tr}_D[Q_{RD}]], \tag{54}$$

$$\begin{bmatrix} \Gamma^{\widetilde{\mathcal{N}}}_{RD} & Q^{\dagger}_{RD} \\ Q_{RD} & \Gamma^{\mathcal{N}}_{RD} \end{bmatrix} \geqslant 0. \tag{55}$$

An alternative method for quantifying the simulation error is to employ the channel infidelity, defined as $1 - F(\mathcal{N}, \widetilde{\mathcal{N}})$. Indeed, we can measure the simulation error as follows, when using a bipartite state $\rho_{\hat{A}\hat{B}}$ and a one-way LOCC channel $\mathcal{L}_{A\hat{A}\hat{B}\to B}$:

$$e^F_{1\mathrm{WL}}(\rho_{\hat{A}\hat{B}}, \mathcal{L}_{A\hat{A}\hat{B}\to B}) \coloneqq 1 - F\big(\mathrm{id}^d_{A\to B}, \widetilde{\mathcal{S}}_{A\to B}\big), \tag{56}$$

where the simulation channel $\widetilde{\mathcal{S}}_{A\to B}$ is defined in (42). By employing (52), we find that

$$e^F_{1\mathrm{WL}}(\rho_{\hat{A}\hat{B}}, \mathcal{L}_{A\hat{A}\hat{B}\to B}) = \sup_{\psi_{RA}}[1 - F(\psi_{RA}, \mathcal{L}_{A\hat{A}\hat{B}\to B}(\psi_{RA} \otimes \rho_{\hat{A}\hat{B}}))], \tag{57}$$

where the optimization is over every pure bipartite state ψ_{RA} with system R isomorphic to the channel input system A. Since we are interested in the minimum possible simulation error, we define

$$e^F_{1\mathrm{WL}}(\rho_{\hat{A}\hat{B}}) \coloneqq \inf_{\mathcal{L}\in 1\mathrm{WL}} e^F_{1\mathrm{WL}}(\rho_{\hat{A}\hat{B}}, \mathcal{L}_{A\hat{A}\hat{B}\to B}). \tag{58}$$

This is the other kind of simulation error on which we are interested in obtaining lower bounds.

C. One-way LOCC simulation of general point-to-point channels

Beyond the case of simulating an ideal channel, more generally we can consider using a resource state $\rho_{\hat{A}\hat{B}}$ along with a one-way LOCC channel $\mathcal{L}_{A\hat{A}\hat{B}\to B}$ in order to simulate a general channel $\mathcal{N}_{A\to B}$. In this case, the simulation channel has the following form:

$$\widetilde{\mathcal{N}}_{A\to B}(\omega_A) \coloneqq \mathcal{L}_{A\hat{A}\hat{B}\to B}(\omega_A \otimes \rho_{\hat{A}\hat{B}}). \tag{59}$$

The simulation error when employing a specific one-way LOCC channel $\mathcal{L}_{A\hat{A}\hat{B}\to B}$ is

$$e_{1\mathrm{WL}}(\mathcal{N}_{A\to B}, \rho_{\hat{A}\hat{B}}, \mathcal{L}_{A\hat{A}\hat{B}\to B}) \coloneqq \tfrac{1}{2}\|\mathcal{N} - \widetilde{\mathcal{N}}\|_{\diamond}, \tag{60}$$

and the simulation error minimized over all possible one-way LOCC channels is

$$e_{1\mathrm{WL}}(\mathcal{N}_{A\to B}, \rho_{\hat{A}\hat{B}}) \coloneqq \inf_{\mathcal{L}\in 1\mathrm{WL}} e_{1\mathrm{WL}}\left(\mathcal{N}_{A\to B}, \rho_{\hat{A}\hat{B}}, \mathcal{L}_{A\hat{A}\hat{B}\to B}\right). \tag{61}$$

We note here that this is a special case of the simulation problem considered in [42, Sec. II].

Alternatively, we can employ the infidelity to quantify the simulation error as follows:

$$e^F_{1\mathrm{WL}}(\mathcal{N}_{A\to B}, \rho_{\hat{A}\hat{B}}, \mathcal{L}_{A\hat{A}\hat{B}\to B}) \coloneqq 1 - F(\mathcal{N}, \widetilde{\mathcal{N}}), \tag{62}$$

$$e^F_{1\mathrm{WL}}(\mathcal{N}_{A\to B}, \rho_{\hat{A}\hat{B}}) \coloneqq \inf_{\mathcal{L}\in 1\mathrm{WL}} e^F_{1\mathrm{WL}}\left(\mathcal{N}_{A\to B}, \rho_{\hat{A}\hat{B}}, \mathcal{L}_{A\hat{A}\hat{B}\to B}\right). \tag{63}$$

D. Equality of simulation errors when simulating the identity channel

Proposition 1 below states that the following equality holds for every bipartite state $\rho_{\hat{A}\hat{B}}$:

$$e_{1\mathrm{WL}}(\rho_{\hat{A}\hat{B}}) = e^F_{1\mathrm{WL}}(\rho_{\hat{A}\hat{B}}). \tag{64}$$

We provide an explicit proof in Appendix B of the Supplemental Material [43]. This equality follows as a consequence of the unitary covariance symmetry of the identity channel being simulated and the fact that an optimal simulating channel should respect the same symmetries. Indeed, consider that the identity channel $\mathrm{id}^d_{A\to B}$ possesses the following unitary covariance symmetry:

$$\mathrm{id}^d_{A\to B} \circ \mathcal{U}_A = \mathcal{U}_B \circ \mathrm{id}^d_{A\to B}, \tag{65}$$

which holds for every unitary channel $\mathcal{U}(\cdot) = U(\cdot)U^{\dagger}$, with U a unitary operator. As a consequence, the theory simplifies in the sense that we need only focus on bounding the simulation error with respect to a single measure. We note here that a similar result was found in [15] for the case of simulating the bipartite swap channel by means of LOCC.

Proposition 1. The optimization problems in (49) and (58), for the error in simulating the identity channel $\mathrm{id}^d_{A\to B}$, simplify as follows:

$$e_{1\mathrm{WL}}(\rho_{\hat{A}\hat{B}}) = e^F_{1\mathrm{WL}}(\rho_{\hat{A}\hat{B}}) \tag{66}$$

$$= 1 - \sup_{K_{\hat{A}\hat{B}}, L_{\hat{A}\hat{B}} \geqslant 0} \mathrm{Tr}[K_{\hat{A}\hat{B}}\rho_{\hat{A}\hat{B}}], \tag{67}$$

subject to $K_{\hat{A}\hat{B}} + L_{\hat{A}\hat{B}} = I_{\hat{A}\hat{B}}$ and the following channel $\mathcal{L}_{A\hat{A}\hat{B}\to B}$ being a one-way LOCC channel:

$$\mathcal{L}_{A\hat{A}\hat{B}\to B}(\omega_{A\hat{A}\hat{B}}) = \mathrm{id}^d_{A\to B}(\mathrm{Tr}_{\hat{A}\hat{B}}[K_{\hat{A}\hat{B}}\omega_{A\hat{A}\hat{B}}]) + \mathcal{D}_{A\to B}(\mathrm{Tr}_{\hat{A}\hat{B}}[L_{\hat{A}\hat{B}}\omega_{A\hat{A}\hat{B}}]), \tag{68}$$

where $\mathcal{D}_{A\to B}$ is the following channel:

$$\mathcal{D}_{A\to B}(\sigma_A) \coloneqq \frac{1}{d^2-1} \sum_{(z,x)\neq(0,0)} W^{z,x}\sigma(W^{z,x})^{\dagger}, \tag{69}$$

and $W^{z,x}$ is defined in (3). The constraint that $\mathcal{L}_{A\hat{A}\hat{B}\to B}$ is a one-way LOCC channel is equivalent to the existence of a positive operator-valued measure (POVM) $\{\Lambda^x_{B\hat{A}}\}_x$ and a set $\{\mathcal{D}^x_{\hat{B}\to B}\}_x$ of channels such that

$$K_{\hat{A}\hat{B}} = \frac{1}{d^2}\sum_x \mathrm{Tr}_B\left[T_B\big(\Lambda^x_{B\hat{A}}\big)\Gamma^{\mathcal{D}^x}_{\hat{B}B}\right], \tag{70}$$

where $\Gamma^{\mathcal{D}^x}_{\hat{B}B}$ is the Choi operator of the channel $\mathcal{D}^x_{\hat{B}\to B}$.

Proof. See Appendix B of the Supplemental Material [43]. ∎

IV. SDP LOWER BOUNDS ON THE PERFORMANCE OF APPROXIMATE TELEPORTATION BASED ON 2-PPT-EXTENDIBILITY

A. SDP lower bound on the error in one-way LOCC simulation of a channel

It is difficult to compute the simulation error $e_{1\mathrm{WL}}(\mathcal{N}_{A\to B}, \rho_{\hat{A}\hat{B}})$ defined in (61) because it is challenging to optimize over the set of one-way LOCC channels [44,45].

Here we enlarge the set of one-way LOCC channels to the set of 2-PPT-extendible bipartite channels, with the goal of simplifying the calculation of the simulation error. The result is that we provide a lower bound on the one-way LOCC simulation error in terms of a semidefinite program, which follows because the set of 2-PPT-extendible channels is specified by semidefinite constraints, as indicated in (31)–(36).

In more detail, recall that a bipartite channel is 2-PPT-extendible if the conditions in (23)–(26) hold. As indicated previously at the end of Sec. II B 5, every one-way LOCC channel is a 2-extendible channel, and the containment is strict. Thus,

$$1\text{WL} \subset 2\text{PE}, \tag{71}$$

where 2PE denotes the set of 2-PPT-extendible channels, as defined in Sec. II B 5.

We can then define the simulation error under 2-PPT-extendible channels, as a semidefinite relaxation of (61), as follows:

$$e_{2\text{PE}}(\mathcal{N}_{A\to B}, \rho_{\hat{A}\hat{B}}) \coloneqq \inf_{\mathcal{K}\in 2\text{PE}} \tfrac{1}{2}\|\mathcal{N} - \widetilde{\mathcal{N}}\|_\diamond, \tag{72}$$

where

$$\widetilde{\mathcal{N}}_{A\to B}(\omega_A) \coloneqq \mathcal{K}_{A\hat{A}\hat{B}\to B}(\omega_A \otimes \rho_{\hat{A}\hat{B}}) \tag{73}$$

and $\mathcal{K}_{A\hat{A}\hat{B}\to B}$ is a 2-PPT-extendible channel, meaning that there exists an extension channel $\mathcal{M}_{A\hat{A}\hat{B}_1\hat{B}_2\to B_1B_2}$ satisfying the following conditions:

$$\text{Tr}_{B_2} \circ \mathcal{M}_{A\hat{A}\hat{B}_1\hat{B}_2\to B_1B_2} = \mathcal{K}_{A\hat{A}\hat{B}_1\to B_1} \otimes \text{Tr}_{\hat{B}_2}, \tag{74}$$

$$\mathcal{M}_{A\hat{A}\hat{B}_1\hat{B}_2\to B_1B_2} \circ \mathcal{F}_{\hat{B}_1\hat{B}_2} = \mathcal{F}_{B_1B_2} \circ \mathcal{M}_{A\hat{A}\hat{B}_1\hat{B}_2\to B_1B_2}, \tag{75}$$

$$T_{B_2} \circ \mathcal{M}_{A\hat{A}\hat{B}_1\hat{B}_2\to B_1B_2} \circ T_{\hat{B}_2} \in \text{CP}, \tag{76}$$

$$\mathcal{M}_{A\hat{A}\hat{B}_1\hat{B}_2\to B_1B_2} \circ T_{A\hat{A}} \in \text{CP}. \tag{77}$$

As a consequence of the containment in (71), the following bound holds:

$$e_{2\text{PE}}(\mathcal{N}_{A\to B}, \rho_{\hat{A}\hat{B}}) \leqslant e_{1\text{WL}}(\mathcal{N}_{A\to B}, \rho_{\hat{A}\hat{B}}). \tag{78}$$

We now show that the simulation error in (72) can be calculated by means of a semidefinite program.

Proposition 2. The simulation error in (72) can be calculated by means of the following semidefinite program:

$$e_{2\text{PE}}(\mathcal{N}_{A\to B}, \rho_{\hat{A}\hat{B}}) = \inf_{\substack{\mu\geqslant 0, Z_{AB}\geqslant 0,\\ M_{A\hat{A}\hat{B}_1B_1\hat{B}_2B_2}\geqslant 0}} \mu, \tag{79}$$

subject to

$$\mu I_A \geqslant Z_A, \tag{80}$$

$$Z_{AB} \geqslant \Gamma^{\mathcal{N}}_{AB} - \text{Tr}_{\hat{A}\hat{B}_1}\left[T_{\hat{A}\hat{B}_1}(\rho_{\hat{A}\hat{B}_1})\frac{M_{A\hat{A}\hat{B}_1B_1}}{d_{\hat{B}}}\right], \tag{81}$$

$$\text{Tr}_{B_1B_2}\left[M_{A\hat{A}\hat{B}_1B_1\hat{B}_2B_2}\right] = I_{A\hat{A}\hat{B}_1\hat{B}_2}, \tag{82}$$

$$\left(\mathcal{F}_{\hat{B}_1\hat{B}_2} \otimes \mathcal{F}_{B_1B_2}\right)\left(M_{A\hat{A}\hat{B}_1B_1\hat{B}_2B_2}\right) = M_{A\hat{A}\hat{B}_1B_1\hat{B}_2B_2}, \tag{83}$$

$$\text{Tr}_{B_2}\left[M_{A\hat{A}\hat{B}_1B_1\hat{B}_2B_2}\right] = \frac{M_{A\hat{A}\hat{B}_1B_1}}{d_{\hat{B}}} \otimes I_{\hat{B}_2}, \tag{84}$$

$$T_{A\hat{A}}\left(M_{A\hat{A}\hat{B}_1B_1\hat{B}_2B_2}\right) \geqslant 0, \tag{85}$$

$$T_{\hat{B}_2B_2}\left(M_{A\hat{A}\hat{B}_1B_1\hat{B}_2B_2}\right) \geqslant 0. \tag{86}$$

The objective function in (79) and the first two constraints in (80) and (81) follow from the semidefinite program in (46) for the normalized diamond distance. The quantity $\text{Tr}_{\hat{A}\hat{B}_1}[T_{\hat{A}\hat{B}_1}(\rho_{\hat{A}\hat{B}_1})\frac{M_{A\hat{A}\hat{B}_1B_1}}{d_{\hat{B}}}]$ in (81) is the Choi operator corresponding to the composition of the appending channel and the simulation channel $\mathcal{K}_{A\hat{A}\hat{B}_1\to B_1}$, with Choi operator $\frac{M_{A\hat{A}\hat{B}_1B_1}}{d_{\hat{B}}}$, where $\mathcal{K}_{A\hat{A}\hat{B}_1\to B_1}$ is the marginal channel of $\mathcal{M}_{A\hat{A}\hat{B}_1\hat{B}_2\to B_1B_2}$, defined as

$$\mathcal{K}_{A\hat{A}\hat{B}_1\to B_1}(\omega_{A\hat{A}\hat{B}_1}) \coloneqq \text{Tr}_{B_2}\left[\mathcal{M}_{A\hat{A}\hat{B}_1\hat{B}_2\to B_1B_2}(\omega_{A\hat{A}\hat{B}_1} \otimes \pi_{\hat{B}_2})\right]. \tag{87}$$

The constraint in (82) forces $\mathcal{M}_{A\hat{A}\hat{B}_1\hat{B}_2\to B_1B_2}$ to be trace preserving, that in (83) forces $\mathcal{M}_{A\hat{A}\hat{B}_1\hat{B}_2\to B_1B_2}$ to be permutation covariant with respect to the B systems [see (75)], and that in (84) forces $\mathcal{M}_{A\hat{A}\hat{B}_1\hat{B}_2\to B_1B_2}$ to be the extension of a marginal channel $\mathcal{K}_{A\hat{A}\hat{B}_1\to B_1}$. The final two PPT constraints are equivalent to the C-PPT-P constraints in (76) and (77), respectively.

B. SDP lower bound on the simulation error of approximate teleportation

The semidefinite program in Proposition 2 can be evaluated for an important case of interest, i.e., when $\mathcal{N}_{A\to B} = \text{id}^d_{A\to B}$. Recall from Sec. III that this special case corresponds to approximate teleportation. The semidefinite program in Proposition 2 is efficiently computable with respect to the dimensions of the systems A, $\hat{A}$, $\hat{B}$, and B. However, it is in our interest to reduce the computational complexity of these optimization tasks even further for this important case, and we can do so by exploiting the unitary covariance symmetry of the identity channel, as stated in (65).

In this section, we provide a semidefinite program for evaluating the simulation error

$$e_{2\text{PE}}(\rho_{\hat{A}\hat{B}}) \equiv e_{2\text{PE}}\left(\text{id}^d_{A\to B}, \rho_{\hat{A}\hat{B}}\right), \tag{88}$$

with reduced complexity, i.e., only polynomial in the dimensions $d_{\hat{A}}$ and $d_{\hat{B}}$ of the resource state $\rho_{\hat{A}\hat{B}}$. We provide a proof of Proposition 3 in Appendix C of the Supplemental Material [43].

Proposition 3. The semidefinite program in Proposition 2, for the special case of simulating the identity channel $\text{id}^d_{A\to B}$, simplifies as follows for $d \geqslant 3$:

$$e_{2\text{PE}}(\rho_{\hat{A}\hat{B}}) = e^F_{2\text{PE}}(\rho_{\hat{A}\hat{B}}) \tag{89}$$

$$= 1 - \sup_{\substack{M^+,M^-,M^0\geqslant 0,\\ M^1,M^2,M^3\in\text{LinOp}}} \text{Tr}\left[T_{\hat{A}\hat{B}_1}(\rho_{\hat{A}\hat{B}_1})\frac{P_{\hat{A}\hat{B}_1\hat{B}_2}}{d_{\hat{B}}}\right], \tag{90}$$

subject to

$$\begin{bmatrix} M^0 + M^3 & M^1 - iM^2 \\ M^1 + iM^2 & M^0 - M^3 \end{bmatrix} \geqslant 0, \tag{91}$$

$$I_{\hat{A}\hat{B}_1\hat{B}_2} = M^+_{\hat{A}\hat{B}_1\hat{B}_2} + M^-_{\hat{A}\hat{B}_1\hat{B}_2} + M^0_{\hat{A}\hat{B}_1\hat{B}_2}, \tag{92}$$

$$M^i_{\hat{A}\hat{B}_1\hat{B}_2} = \mathcal{F}_{\hat{B}_1\hat{B}_2}\left(M^i_{\hat{A}\hat{B}_1\hat{B}_2}\right) \quad \forall i \in \{+, -, 0, 1\}, \tag{93}$$

$$M^j_{\hat{A}\hat{B}_1\hat{B}_2} = -\mathcal{F}_{\hat{B}_1\hat{B}_2}\left(M^j_{\hat{A}\hat{B}_1\hat{B}_2}\right) \quad \forall j \in \{2,3\}, \tag{94}$$

$$P_{\hat{A}\hat{B}_1\hat{B}_2} = \frac{1}{d_{\hat{B}}} \operatorname{Tr}_{\hat{B}_2}\left[P_{\hat{A}\hat{B}_1\hat{B}_2}\right] \otimes I_{\hat{B}_2}, \tag{95}$$

$$P_{\hat{A}\hat{B}_1\hat{B}_2} := \frac{1}{2d}[dM^0 + M^1 + \sqrt{d^2-1}\, M^2], \tag{96}$$

$$T_{\hat{A}}\left(\frac{2M^+_{\hat{A}\hat{B}_1\hat{B}_2}}{d+2} + M^0_{\hat{A}\hat{B}_1\hat{B}_2} + M^1_{\hat{A}\hat{B}_1\hat{B}_2}\right) \geqslant 0, \tag{97}$$

$$T_{\hat{A}}\left(\frac{2M^-_{\hat{A}\hat{B}_1\hat{B}_2}}{d-2} + M^1_{\hat{A}\hat{B}_1\hat{B}_2} - M^0_{\hat{A}\hat{B}_1\hat{B}_2}\right) \geqslant 0, \tag{98}$$

$$\begin{bmatrix} G^0 + G^3 & G^1 - iG^2 \\ G^1 + iG^2 & G^0 - G^3 \end{bmatrix} \geqslant 0, \tag{99}$$

$$G^0_{\hat{A}\hat{B}_1\hat{B}_2} := T_{\hat{A}}\left(M^+ + M^- + \frac{M^0 - dM^1}{2}\right), \tag{100}$$

$$G^1_{\hat{A}\hat{B}_1\hat{B}_2} := T_{\hat{A}}\left(M^+ - M^- + \frac{M^1 - dM^0}{2}\right), \tag{101}$$

$$G^2_{\hat{A}\hat{B}_1\hat{B}_2} := \frac{\sqrt{3(d^2-1)}}{2} T_{\hat{A}}\left(M^2_{\hat{A}\hat{B}_1\hat{B}_2}\right), \tag{102}$$

$$G^3_{\hat{A}\hat{B}_1\hat{B}_2} := \frac{\sqrt{3(d^2-1)}}{2} T_{\hat{A}}\left(M^3_{\hat{A}\hat{B}_1\hat{B}_2}\right). \tag{103}$$

$$T_{\hat{A}\hat{B}_1}\left(\frac{dM^+}{d+2} + M^- + \frac{dM^0 - M^1 - \sqrt{d^2-1}\, M^2}{2}\right) \geqslant 0, \tag{104}$$

$$T_{\hat{A}\hat{B}_1}\left(M^+ + \frac{dM^-}{d-2} - \frac{dM^0 - M^1 - \sqrt{d^2-1}\, M^2}{2}\right) \geqslant 0, \tag{105}$$

$$\begin{bmatrix} E^0 + E^3 & E^1 - iE^2 \\ E^1 + iE^2 & E^0 - E^3 \end{bmatrix} \geqslant 0, \tag{106}$$

$$E^0_{\hat{A}\hat{B}_1\hat{B}_2} := \frac{T_{\hat{A}\hat{B}_1}\left(d(M^+ - M^-) + \frac{L^0}{2}\right)}{d^2-1}, \tag{107}$$

$$E^1_{\hat{A}\hat{B}_1\hat{B}_2} := \frac{T_{\hat{A}\hat{B}_1}\left(-M^+ + M^- + \frac{L^1}{2}\right)}{d^2-1}, \tag{108}$$

$$E^2_{\hat{A}\hat{B}_1\hat{B}_2} := \frac{T_{\hat{A}\hat{B}_1}\left(M^+ - M^- + \frac{L^2}{2}\right)}{\sqrt{d^2-1}}, \tag{109}$$

$$E^3_{\hat{A}\hat{B}_1\hat{B}_2} := T_{\hat{A}\hat{B}_1}\left(M^3_{\hat{A}\hat{B}_1\hat{B}_2}\right), \tag{110}$$

$$L^0 := (d^2-2)M^0 + dM^1 + d\sqrt{d^2-1}\, M^2, \tag{111}$$

$$L^1 := dM^0 + (2d^2-3)M^1 - \sqrt{d^2-1}\, M^2, \tag{112}$$

$$L^2 := M^1 - dM^0 - \sqrt{d^2-1}\, M^2. \tag{113}$$

For the case of $d = 2$, the SDP is the same, with the exception that we set $M^-_{\hat{A}\hat{B}_1\hat{B}_2} = 0$ and the constraints in (98) and (105) are not used.

Proof. See Appendix C of the Supplemental Material [43]. ■

Remark 4. The SDP in the statement of Proposition 3 is rather lengthy, and so we provide some explanation here. The constraint in (91) and the constraints $M^+, M^-, M^0 \geqslant 0$ in (90) correspond to the constraint of complete positivity in (79) (i.e., $M_{A\hat{A}\hat{B}_1B_1\hat{B}_2B_2} \geqslant 0$). The constraint in (92) corresponds to the constraint of trace preservation in (82). The constraints in (93)–(94) correspond to the permutation covariance constraint in (83). The constraint in (95) corresponds to the nonsignaling constraint in (84). The constraints in (97)–(99) correspond to the PPT constraint in (85), and the constraints in (104)–(106) correspond to the PPT constraint in (86).

Remark 5. Even though the number of constraints in the SDP above appears to increase when compared with the SDP from Proposition 2, we note that the runtime of the SDP above is significantly reduced because the size of the matrices involved in each of the constraints is much smaller. This is the main advantage conferred by incorporating unitary covariance symmetry of the identity channel.

If we only optimized over the larger set of 2-extendible channels instead of the set of 2-PPT-extendible channels, the SDP would be much simpler, given by (90)–(96). However, optimizing over the smaller set of 2-PPT-extendible channels gives tighter bounds at a marginal increase in computational cost, and thus we also include the PPT constraints in (97)–(99) and (104)–(106).

V. BACKGROUND ON SUPERCHANNELS

This section constitutes the beginning of the second contribution of our paper, regarding lower bounds on the error in channel simulation and approximate quantum error correction. We begin by reviewing the theory of superchannels, as well as particular examples of them relevant to the aforementioned applications.

A. Basics of superchannels

A superchannel $\Theta \equiv \Theta_{(A\to B)\to(C\to D)}$ is a physical transformation of a channel $\mathcal{N}_{A\to B}$ that accepts as input the channel $\mathcal{N}_{A\to B}$ and outputs a channel with input system C and output system D. Mathematically, a superchannel is a linear map that preserves the set of quantum channels, even when the quantum channel is an arbitrary bipartite channel with external input and output systems that are arbitrarily large. Superchannels are thus completely CPTP preserving in this sense. A general theory of superchannels was introduced in [21] and developed further in [46–48].

In more detail, let us denote the output of a superchannel Θ by $\mathcal{K}_{C\to D}$, so that

$$\Theta_{(A\to B)\to(C\to D)}(\mathcal{N}_{A\to B}) = \mathcal{K}_{C\to D}. \tag{114}$$

The superchannel $\Theta_{(A\to B)\to(C\to D)}$ is completely CPTP preserving in the sense that the following output map

$$(\mathrm{id}_{(R)\to(R)} \otimes \Theta_{(A\to B)\to(C\to D)})(\mathcal{M}_{RA\to RB}) \tag{115}$$

is a quantum channel for every input quantum channel $\mathcal{M}_{RA\to RB}$, where $\mathrm{id}_{(R)\to(R)}$ denotes the identity superchannel [21].

The fundamental theorem of superchannels from [21] is that $\Theta_{(A\to B)\to(C\to D)}$ has a physical realization in terms of a preprocessing channel $\mathcal{E}_{C\to AQ}$ and a postprocessing channel

$\mathcal{D}_{BQ\to D}$ as follows:

$$\Theta_{(A\to B)\to(C\to D)}(\mathcal{N}_{A\to B}) = \mathcal{D}_{BQ\to D}\circ\mathcal{N}_{A\to B}\circ\mathcal{E}_{C\to AQ}, \tag{116}$$

where Q is a quantum memory system. Furthermore, every superchannel $\Theta_{(A\to B)\to(C\to D)}$ is in one-to-one correspondence with a bipartite channel of the following form:

$$\mathcal{P}_{CB\to AD} := \mathcal{D}_{BQ\to D}\circ\mathcal{E}_{C\to AQ}. \tag{117}$$

Note that $\mathcal{P}_{CB\to AD}$ is completely positive, trace preserving, and obeys the following nonsignaling constraint:

$$\mathrm{Tr}_D\circ\mathcal{P}_{CB\to AD} = \mathrm{Tr}_D\circ\mathcal{P}_{CB\to AD}\circ\mathcal{R}_B^{\pi}, \tag{118}$$

where the replacer channel $\mathcal{R}_B^{\pi}$ is defined in (13). Related to this, $\Gamma^{\mathcal{P}}_{CBAD}$ is the Choi operator of a superchannel if and only if it satisfies the following constraints:

$$\Gamma^{\mathcal{P}}_{CBAD} \geqslant 0, \tag{119}$$

$$\mathrm{Tr}_{AD}\left[\Gamma^{\mathcal{P}}_{CBAD}\right] = I_{CB}, \tag{120}$$

$$\mathrm{Tr}_{D}\left[\Gamma^{\mathcal{P}}_{CBAD}\right] = \frac{1}{d_B}\mathrm{Tr}_{BD}\left[\Gamma^{\mathcal{P}}_{CBAD}\right]\otimes I_B. \tag{121}$$

The first two constraints correspond to complete positivity and trace preservation, respectively, and the last constraint is a nonsignaling constraint corresponding to $\mathcal{P}_{CB\to AD}$ having the factorization in (117), so that $\mathcal{P}_{CB\to AD}$ is in correspondence with a superchannel. To determine the Choi operator for the output channel $\mathcal{K}_{C\to D}$ in (114), we can use the following propagation rule [21,48]:

$$\Gamma^{\mathcal{K}}_{CD} = \mathrm{Tr}_{AB}\left[T_{AB}\left(\Gamma^{\mathcal{N}}_{AB}\right)\Gamma^{\mathcal{P}}_{CBAD}\right], \tag{122}$$

where $\Gamma^{\mathcal{P}}_{CBAD}$ is the Choi operator of $\mathcal{P}_{CB\to AD}$ and $\Gamma^{\mathcal{N}}_{AB}$ is the Choi operator of $\mathcal{N}_{A\to B}$.

B. One-way LOCC superchannels

A superchannel $\Lambda \equiv \Lambda_{(A\to B)\to(C\to D)}$ is implementable by one-way LOCC if it can be written in the following form:

$$\Lambda(\mathcal{N}_{A\to B}) := \sum_x \mathcal{D}^x_{B\to D}\circ\mathcal{N}_{A\to B}\circ\mathcal{E}^x_{C\to A}, \tag{123}$$

where $\{\mathcal{E}^x_{C\to A}\}_x$ is a set of completely positive maps such that the sum map $\sum_x \mathcal{E}^x_{C\to A}$ is trace preserving and $\{\mathcal{D}^x_{B\to D}\}_x$ is a set of quantum channels. This is equivalent to the quantum memory system Q in (116) being a classical system X, with

$$\mathcal{E}_{C\to AX}(\rho_C) := \sum_x \mathcal{E}^x_{C\to A}(\rho_C)\otimes|x\rangle\langle x|_X, \tag{124}$$

$$\mathcal{D}_{BX\to D}(\omega_{BX}) := \sum_x \mathcal{D}^x_{B\to D}(\langle x|_X\omega_{BX}|x\rangle_X), \tag{125}$$

so that

$$\Lambda(\mathcal{N}_{A\to B}) = \mathcal{D}_{BX\to D}\circ\mathcal{N}_{A\to B}\circ\mathcal{E}_{C\to AX}. \tag{126}$$

In this case, the bipartite channel in (117), but corresponding to Λ in (123), becomes the following one-way LOCC channel:

$$\mathcal{L}_{CB\to AD} := \sum_x \mathcal{E}^x_{C\to A}\otimes\mathcal{D}^x_{B\to D}. \tag{127}$$

Thus, the set of one-way LOCC superchannels is in direct correspondence with the set of one-way LOCC bipartite channels.

C. LOCR superchannels

A superchannel $\Upsilon \equiv \Upsilon_{(A\to B)\to(C\to D)}$ is implementable by local operations and common randomness (LOCR) if it can be written in the following form:

$$\Upsilon(\mathcal{N}_{A\to B}) := \sum_y p(y)\mathcal{D}^y_{B\to D}\circ\mathcal{N}_{A\to B}\circ\mathcal{E}^y_{C\to A}, \tag{128}$$

where $\{p(y)\}_y$ is a probability distribution and $\{\mathcal{E}^y_{C\to A}\}_y$ and $\{\mathcal{D}^y_{B\to D}\}_y$ are sets of quantum channels. In more detail, the superchannel $\Upsilon_{(A\to B)\to(C\to D)}$ can be realized as

$$\Upsilon(\mathcal{N}_{A\to B}) = \mathcal{D}_{BY_B\to D}\circ\mathcal{N}_{A\to B}\circ\mathcal{E}_{CY_A\to A}\circ\mathcal{P}_{Y_AY_B}, \tag{129}$$

where $\mathcal{P}_{Y_AY_B}$ is a preparation channel that prepares the common randomness state

$$\sum_y p(y)|y\rangle\langle y|_{Y_A}\otimes|y\rangle\langle y|_{Y_B}, \tag{130}$$

and the channels $\mathcal{E}_{CY_A\to A}$ and $\mathcal{D}_{BY_B\to D}$ are defined as

$$\mathcal{E}_{CY_A\to A}(\rho_{CY_A}) := \sum_y \mathcal{E}^y_{C\to A}\left(\langle y|_{Y_A}\rho_{CY_A}|y\rangle_{Y_A}\right), \tag{131}$$

$$\mathcal{D}_{BY_B\to D}(\omega_{BY_B}) := \sum_y \mathcal{D}^y_{B\to D}\left(\langle y|_{Y_B}\omega_{BY_B}|y\rangle_{Y_B}\right). \tag{132}$$

In this case, the bipartite channel in (117), but corresponding to Υ in (128), becomes the following LOCR bipartite channel:

$$\mathcal{C}_{CB\to AD} := \sum_y p(y)\mathcal{E}^y_{C\to A}\otimes\mathcal{D}^y_{B\to D}. \tag{133}$$

Thus, the set of LOCR superchannels is in direct correspondence with the set of LOCR bipartite channels.

D. 2-extendible superchannels

A superchannel $\Theta_{(A\to B)\to(C\to D)}$ is defined to be 2-extendible if there exists an extension channel $\mathcal{M}_{CB_1B_2\to AD_1D_2}$ of its corresponding bipartite channel $\mathcal{P}_{CB\to AD}$ that obeys the conditions in (10) and (11). Furthermore, due to the fact that (10) and (11) imply (12), there is no need to explicitly indicate that (118) holds. 2-extendible superchannels were considered in [18], but this terminology was not employed there.

The specific constraints on the Choi operator of $\mathcal{M}_{CB_1B_2\to AD_1D_2}$ are precisely the same as those in (14)–(17), with the identifications $C\leftrightarrow A$, $B\leftrightarrow B$, $A\leftrightarrow A'$, and $D\leftrightarrow B'$. Explicitly, a superchannel $\Theta_{(A\to B)\to(C\to D)}$ is 2-extendible if the Choi operator $\Gamma^{\mathcal{P}}_{CBAD}$ of its corresponding bipartite channel $\mathcal{P}_{CB\to AD}$ satisfies the following conditions: there exists a Hermitian operator $\Gamma^{\mathcal{M}}_{CB_1B_2AD_1D_2}$ such that

$$\left(\mathcal{F}_{B_1B_2}\otimes\mathcal{F}_{D_1D_2}\right)\left(\Gamma^{\mathcal{M}}_{CB_1B_2AD_1D_2}\right) = \Gamma^{\mathcal{M}}_{CB_1B_2AD_1D_2}, \tag{134}$$

$$\mathrm{Tr}_{D_2}\left[\Gamma^{\mathcal{M}}_{CB_1B_2AD_1D_2}\right] = \Gamma^{\mathcal{P}}_{CB_1AD_1}\otimes I_{B_2}, \tag{135}$$

$$\Gamma^{\mathcal{M}}_{CB_1B_2AD_1D_2} \geqslant 0, \tag{136}$$

$$\mathrm{Tr}_{AD_1D_2}\left[\Gamma^{\mathcal{M}}_{CB_1B_2AD_1D_2}\right] = I_{CB_1B_2}. \tag{137}$$

Every one-way LOCC superchannel is 2-extendible.

E. Completely PPT preserving superchannels

A superchannel $\Theta_{(A\to B)\to(C\to D)}$ is C-PPT-P if its corresponding bipartite channel $\mathcal{P}_{CB\to AD}$ in (117) is C-PPT-P and obeys the nonsignaling constraint in (118) [31]. This implies the following for its Choi operator $\Gamma^{\mathcal{P}}_{CBAD}$:

$$\Gamma^{\mathcal{P}}_{CBAD} \geqslant 0, \tag{138}$$

$$\operatorname{Tr}_{AD}\left[\Gamma^{\mathcal{P}}_{CBAD}\right] = I_{CB}, \tag{139}$$

$$\operatorname{Tr}_{D}\left[\Gamma^{\mathcal{P}}_{CBAD}\right] = \frac{1}{d_B}\operatorname{Tr}_{BD}\left[\Gamma^{\mathcal{P}}_{CBAD}\right]\otimes I_B, \tag{140}$$

$$T_{BD}\left(\Gamma^{\mathcal{P}}_{CBAD}\right) \geqslant 0. \tag{141}$$

F. 2-PPT-extendible superchannels

A superchannel $\Theta_{(A\to B)\to(C\to D)}$ is 2-PPT-extendible if its corresponding bipartite channel $\mathcal{P}_{CB\to AD}$ in (117) is 2-PPT-extendible. Again, there is no need to explicitly indicate that (118) holds. The following conditions hold for the Choi operator $\Gamma^{\mathcal{P}}_{CBAD}$ of a 2-PPT-extendible superchannel: there exists a Hermitian operator $\Gamma^{\mathcal{M}}_{CB_1B_2AD_1D_2}$ such that (134)–(137) hold, as well as

$$T_{B_2D_2}\left(\Gamma^{\mathcal{M}}_{CB_1B_2AD_1D_2}\right) \geqslant 0,$$
$$T_{CA}\left(\Gamma^{\mathcal{M}}_{CB_1B_2AD_1D_2}\right) \geqslant 0.$$

Similar to what was already discussed in Sec. II B 5, the following constraints are redundant:

$$T_{B_1D_1}\left(\Gamma^{\mathcal{M}}_{CB_1B_2AD_1D_2}\right) \geqslant 0, \tag{142}$$

$$T_{CAB_2D_2}\left(\Gamma^{\mathcal{M}}_{CB_1B_2AD_1D_2}\right) \geqslant 0, \tag{143}$$

$$T_{CAB_1D_1}\left(\Gamma^{\mathcal{M}}_{CB_1B_2AD_1D_2}\right) \geqslant 0, \tag{144}$$

$$T_{B_1D_1B_2D_2}\left(\Gamma^{\mathcal{M}}_{CB_1B_2AD_1D_2}\right) \geqslant 0. \tag{145}$$

Note that every one-way LOCC superchannel is 2-PPT-extendible.

G. 2-PPT-extendible nonsignaling superchannels

Finally, we can impose an additional nonsignaling constraint on 2-PPT-extendible superchannels, such that the extension of its corresponding bipartite channel is nonsignaling from Alice to both Bobs. The additional constraint on the Choi operator $\Gamma^{\mathcal{M}}_{CB_1B_2AD_1D_2}$ of the extension channel $\mathcal{M}_{CB_1B_2\to AD_1D_2}$ is as follows:

$$\operatorname{Tr}_{A}\left[\Gamma^{\mathcal{M}}_{CB_1B_2AD_1D_2}\right] = \frac{1}{d_C}\operatorname{Tr}_{AC}\left[\Gamma^{\mathcal{M}}_{CB_1B_2AD_1D_2}\right]\otimes I_C. \tag{146}$$

Every LOCR superchannel is nonsignaling and 2-PPT-extendible, which follows from definitions and the form of the corresponding bipartite channel in (133). This fact plays an important role in our analysis of approximate quantum error correction. In more detail, we obtain our tightest lower bound on the simulation error of approximate quantum error correction by relaxing the set of LOCR superchannels to the set of nonsignaling and 2-PPT-extendible superchannels. We note here that this approach was already considered in [18], and our main contribution here is to employ unitary covariance symmetry of the identity channel to reduce the complexity of the SDPs from that work.

VI. QUANTIFYING THE PERFORMANCE OF APPROXIMATE QUANTUM ERROR CORRECTION

A. Quantifying simulation error with normalized diamond distance and channel infidelity

In approximate quantum error correction [49] or quantum communication [2], the resource available is a quantum channel $\mathcal{N}_{\hat{A}\to\hat{B}}$ and the goal is to use it, along with an encoding channel $\mathcal{E}_{A\to\hat{A}}$ and a decoding channel $\mathcal{D}_{\hat{B}\to B}$, to simulate a d-dimensional identity channel $\mathrm{id}^d_{A\to B}$. We can use the normalized diamond distance to quantify the error for a fixed encoding and decoding, as follows:

$$e(\mathcal{N}_{\hat{A}\to\hat{B}}, (\mathcal{E}_{A\to\hat{A}}, \mathcal{D}_{\hat{B}\to B})) := \tfrac{1}{2}\left\|\mathrm{id}^d_{A\to B} - \mathcal{D}_{\hat{B}\to B}\circ\mathcal{N}_{\hat{A}\to\hat{B}}\circ\mathcal{E}_{A\to\hat{A}}\right\|_\diamond. \tag{147}$$

By minimizing over all encodings and decodings, we arrive at the error in using the channel $\mathcal{N}_{\hat{A}\to\hat{B}}$ to simulate the identity channel:

$$e(\mathcal{N}_{\hat{A}\to\hat{B}}) := \inf_{(\mathcal{E},\mathcal{D})} e(\mathcal{N}_{\hat{A}\to\hat{B}}, (\mathcal{E}_{A\to\hat{A}}, \mathcal{D}_{\hat{B}\to B})). \tag{148}$$

We can alternatively employ channel infidelity to quantify the error:

$$e^F(\mathcal{N}_{\hat{A}\to\hat{B}}, (\mathcal{E}_{A\to\hat{A}}, \mathcal{D}_{\hat{B}\to B})) := 1 - F\left(\mathrm{id}^d_{A\to B}, \mathcal{D}_{\hat{B}\to B}\circ\mathcal{N}_{\hat{A}\to\hat{B}}\circ\mathcal{E}_{A\to\hat{A}}\right), \tag{149}$$

$$e^F(\mathcal{N}_{\hat{A}\to\hat{B}}) := \inf_{(\mathcal{E},\mathcal{D})} e^F(\mathcal{N}_{\hat{A}\to\hat{B}}, (\mathcal{E}_{A\to\hat{A}}, \mathcal{D}_{\hat{B}\to B})). \tag{150}$$

Note that the transformation of the channel given by

$$\mathcal{D}_{\hat{B}\to B}\circ\mathcal{N}_{\hat{A}\to\hat{B}}\circ\mathcal{E}_{A\to\hat{A}} \tag{151}$$

is a superchannel, as discussed in Sec. V, with corresponding bipartite channel

$$\mathcal{P}_{A\hat{B}\to\hat{A}B} := \mathcal{E}_{A\to\hat{A}}\otimes\mathcal{D}_{\hat{B}\to B}. \tag{152}$$

As this bipartite channel is a product channel, it is contained within the set of LOCR superchannels, which in turn is contained in the set of one-way LOCC superchannels.

By supplementing the encoding and decoding with common randomness, the resulting error correction scheme $\Upsilon \equiv \Upsilon_{(\hat{A}\to\hat{B})\to(A\to B)}$ realizes the following simulation channel:

$$\Upsilon(\mathcal{N}_{\hat{A}\to\hat{B}}) := \sum_y p(y)\mathcal{D}^y_{\hat{B}\to B}\circ\mathcal{N}_{\hat{A}\to\hat{B}}\circ\mathcal{E}^y_{A\to\hat{A}}, \tag{153}$$

where $\{p(y)\}_y$ is a probability distribution and $\{\mathcal{E}^y_{A\to\hat{A}}\}_y$ and $\{\mathcal{D}^y_{\hat{B}\to B}\}_y$ are sets of quantum channels. Recall from Sec. V C that Υ is an LOCR superchannel, and let LOCR denote the set of all LOCR superchannels. Then we can quantify the simulation error under LOCR in a manner similar to Sec. III A: we can use the normalized diamond distance to quantify the error for a fixed LOCR superchannel Υ, as follows:

$$e_{\mathrm{LOCR}}(\mathcal{N}_{\hat{A}\to\hat{B}}, \Upsilon_{(\hat{A}\to\hat{B})\to(A\to B)}) := \tfrac{1}{2}\left\|\mathrm{id}^d_{A\to B} - \Upsilon_{(\hat{A}\to\hat{B})\to(A\to B)}(\mathcal{N}_{\hat{A}\to\hat{B}})\right\|_\diamond. \tag{154}$$

By minimizing over all such superchannels, we arrive at the error in using the channel $\mathcal{N}_{\hat{A}\to\hat{B}}$ to simulate the identity channel:

$$e_{\mathrm{LOCR}}(\mathcal{N}_{\hat{A}\to\hat{B}}) \coloneqq \inf_{\Upsilon\in\mathrm{LOCR}} e(\mathcal{N}_{\hat{A}\to\hat{B}}, \Upsilon_{(\hat{A}\to\hat{B})\to(A\to B)}). \quad (155)$$

As before, we can alternatively employ channel infidelity to quantify the error:

$$e^F_{\mathrm{LOCR}}(\mathcal{N}_{\hat{A}\to\hat{B}}, \Upsilon_{(\hat{A}\to\hat{B})\to(A\to B)}) \coloneqq 1 - F\big(\mathrm{id}^d_{A\to B}, \Upsilon_{(\hat{A}\to\hat{B})\to(A\to B)}(\mathcal{N}_{\hat{A}\to\hat{B}})\big), \quad (156)$$

$$e^F_{\mathrm{LOCR}}(\mathcal{N}_{\hat{A}\to\hat{B}}) \coloneqq \inf_{\Upsilon\in\mathrm{LOCR}} e^F_{\mathrm{LOCR}}(\mathcal{N}_{\hat{A}\to\hat{B}}, \Upsilon_{(\hat{A}\to\hat{B})\to(A\to B)}). \quad (157)$$

However, we have the following:

Proposition 6. For a channel $\mathcal{N}_{\hat{A}\to\hat{B}}$, the LOCR simulation errors defined from normalized diamond distance and channel infidelity are equal to each other:

$$e_{\mathrm{LOCR}}(\mathcal{N}_{\hat{A}\to\hat{B}}) = e^F_{\mathrm{LOCR}}(\mathcal{N}_{\hat{A}\to\hat{B}}). \quad (158)$$

Proof. The proof of this equality is similar to the proof of Proposition 1, following again from the symmetry of the target channel, which is an identity channel having the symmetry in (65), and the fact that a channel twirl can be implemented by means of LOCR. Note that a channel twirl of a channel $\mathcal{M}_{A\to B}$ has the following form:

$$\int dU\, \mathcal{U}^\dagger_B \circ \mathcal{M}_{A\to B} \circ \mathcal{U}_A, \quad (159)$$

where $\mathcal{U}$ is a unitary channel. ■

By exploiting the fact that a superchannel of the form in (151) is contained in the set of LOCR superchannels, the following inequality holds:

$$e_{\mathrm{LOCR}}(\mathcal{N}_{\hat{A}\to\hat{B}}) \leqslant \min\{e(\mathcal{N}_{\hat{A}\to\hat{B}}), e^F(\mathcal{N}_{\hat{A}\to\hat{B}})\}. \quad (160)$$

It is unclear if $e(\mathcal{N}_{\hat{A}\to\hat{B}})$ is equal to $e^F(\mathcal{N}_{\hat{A}\to\hat{B}})$ in general: a critical aspect of the proof of Proposition 6 is the fact that LOCR superchannels are allowed for free, so that the symmetrizing twirling superchannel can be used. In the unassisted setting, we cannot use twirling because it is an LOCR superchannel and thus not allowed for free.

Recall again that the identity channel $\mathrm{id}^d_{A\to B}$ possesses the unitary covariance symmetry in (65). Considering this leads to the following proposition:

Proposition 7. The optimization problems in (155) and (157), for the error in simulating the identity channel $\mathrm{id}^d_{A\to B}$, simplify as follows:

$$e_{\mathrm{LOCR}}(\mathcal{N}_{\hat{A}\to\hat{B}}) = e^F_{\mathrm{LOCR}}(\mathcal{N}_{\hat{A}\to\hat{B}}) \quad (161)$$

$$= 1 - \sup_{\mathcal{P}} E_F(\mathcal{N}_{\hat{A}\to\hat{B}}; \mathcal{P}), \quad (162)$$

where the optimization in (162) is over every LOCR protocol $\mathcal{P}$, defined as

$$\mathcal{P} \coloneqq \big\{\big(p(y), \mathcal{E}^y_{A\to\hat{A}}, \mathcal{D}^y_{\hat{B}\to B}\big)\big\}_y, \quad (163)$$

and $E_F(\mathcal{N}_{\hat{A}\to\hat{B}}; \mathcal{P}) \in [0, 1]$ is the entanglement fidelity:

$$E_F \equiv E_F(\mathcal{N}_{\hat{A}\to\hat{B}}; \mathcal{P}) \quad (164)$$

$$\coloneqq \sum_y p(y) \operatorname{Tr}\big[\Phi^d_{AB}\big(\mathcal{D}^y_{\hat{B}\to B} \circ \mathcal{N}_{\hat{A}\to\hat{B}} \circ \mathcal{E}^y_{A\to\hat{A}}\big)\big(\Phi^d_{AB}\big)\big]. \quad (165)$$

An optimal LOCR simulation channel for both $e_{\mathrm{LOCR}}(\mathcal{N}_{\hat{A}\to\hat{B}})$ and $e^F_{\mathrm{LOCR}}(\mathcal{N}_{\hat{A}\to\hat{B}})$ has the following form:

$$E_F\, \mathrm{id}^d_{A\to B} + (1 - E_F)\mathcal{D}_{A\to B}, \quad (166)$$

where $\mathcal{D}_{A\to B}$ is the channel defined in (69). Thus, the LOCR simulation channel applies the identity channel $\mathrm{id}^d_{A\to B}$ with probability E_F and the randomizing channel $\mathcal{D}_{A\to B}$ with probability $1 - E_F$.

Proof. See Appendix D of the Supplemental Material [43]. ■

B. LOCR simulation of general point-to-point channels

We can use a point-to-point channel $\mathcal{N}_{\hat{A}\to\hat{B}}$, along with LOCR, to simulate another general point-to-point channel $\mathcal{O}_{A\to B}$. In this case, the simulation channel $\widetilde{\mathcal{O}}_{A\to B}$ has the form

$$\widetilde{\mathcal{O}}_{A\to B} \coloneqq \Upsilon_{(\hat{A}\to\hat{B})\to(A\to B)}(\mathcal{N}_{\hat{A}\to\hat{B}}), \quad (167)$$

where $\Upsilon_{(\hat{A}\to\hat{B})\to(A\to B)}$ is an LOCR superchannel, as discussed in Sec. V C. The simulation error when employing a specific LOCR superchannel $\Upsilon_{(\hat{A}\to\hat{B})\to(A\to B)}$ is

$$e_{\mathrm{LOCR}}(\mathcal{O}_{A\to B}, \mathcal{N}_{\hat{A}\to\hat{B}}, \Upsilon_{(\hat{A}\to\hat{B})\to(A\to B)}) \coloneqq \tfrac{1}{2}\|\mathcal{O}_{A\to B} - \widetilde{\mathcal{O}}_{A\to B}\|_\diamond, \quad (168)$$

and the simulation error minimized over all possible LOCR superchannels is

$$e_{\mathrm{LOCR}}(\mathcal{O}_{A\to B}, \mathcal{N}_{\hat{A}\to\hat{B}}) \coloneqq \inf_{\Upsilon\in\mathrm{LOCR}} e_{\mathrm{LOCR}}(\mathcal{O}_{A\to B}, \mathcal{N}_{\hat{A}\to\hat{B}}, \Upsilon_{(\hat{A}\to\hat{B})\to(A\to B)}). \quad (169)$$

Again we can alternatively consider quantifying simulation error in terms of the channel infidelity:

$$e^F_{\mathrm{LOCR}}(\mathcal{O}_{A\to B}, \mathcal{N}_{\hat{A}\to\hat{B}}, \Upsilon_{(\hat{A}\to\hat{B})\to(A\to B)}) \coloneqq 1 - F(\mathcal{O}_{A\to B}, \widetilde{\mathcal{O}}_{A\to B}), \quad (170)$$

$$e^F_{\mathrm{LOCR}}(\mathcal{O}_{A\to B}, \mathcal{N}_{\hat{A}\to\hat{B}}) \coloneqq \inf_{\Upsilon\in\mathrm{LOCR}} e^F_{\mathrm{LOCR}}(\mathcal{O}_{A\to B}, \mathcal{N}_{\hat{A}\to\hat{B}}, \Upsilon_{(\hat{A}\to\hat{B})\to(A\to B)}). \quad (171)$$

VII. SDP LOWER BOUNDS ON THE PERFORMANCE OF APPROXIMATE QUANTUM ERROR CORRECTION BASED ON 2-PPT EXTENDIBILITY AND NONSIGNALING CONSTRAINTS

A. SDP lower bound on the error in LOCR simulation of a channel

Using (169) to calculate the simulation error, we again encounter an intractable optimization task. Employing the same idea from Sec. IV A, we enlarge the set of LOCR superchannels to 2-PPT-extendible, nonsignaling superchannels (abbreviated henceforth as 2PENS). As noted in Sec. V G, the 2PENS set strictly contains the set of LOCR superchannels.

Thus, we can obtain a lower bound on the simulation error by optimizing over all 2PENS superchannels. We define the simulation error under 2PENS superchannels as

$$e_{\text{2PENS}}(\mathcal{O}_{A\to B}, \mathcal{N}_{\hat{A}\to\hat{B}}) \coloneqq \inf_{\Upsilon\in\text{2PENS}} \tfrac{1}{2}\|\mathcal{O}_{A\to B} - \widetilde{\mathcal{O}}_{A\to B}\|_{\diamond}, \tag{172}$$

where $\widetilde{\mathcal{O}}_{A\to B}$ is defined in (167).

As a result of the strict containment

$$\text{LOCR} \subset \text{2PENS}, \tag{173}$$

we have the relation

$$e_{\text{2PENS}}(\mathcal{O}_{A\to B}, \mathcal{N}_{\hat{A}\to\hat{B}}) \leqslant e_{\text{LOCR}}(\mathcal{O}_{A\to B}, \mathcal{N}_{\hat{A}\to\hat{B}}). \tag{174}$$

We now state that the simulation error in (172) can be calculated by means of a semidefinite program.

Proposition 8. The simulation error in (172) can be calculated by means of the following semidefinite program:

$$e_{\text{2PENS}}(\mathcal{O}_{A\to B}, \mathcal{N}_{\hat{A}\to\hat{B}}) = \inf_{\substack{\mu\geqslant 0, Z_{AB}\geqslant 0,\\ M_{A\hat{A}\hat{B}_1B_1\hat{B}_2B_2}\geqslant 0}} \mu, \tag{175}$$

subject to

$$\mu I_A \geqslant Z_A, \tag{176}$$

$$Z_{AB} \geqslant \Gamma^{\mathcal{O}}_{AB} - \text{Tr}_{\hat{A}\hat{B}_1}\left[T_{\hat{A}\hat{B}_1}\left(\Gamma^{\mathcal{N}}_{\hat{A}\hat{B}_1}\right) M_{A\hat{A}\hat{B}_1B_1}/d_{\hat{B}}\right], \tag{177}$$

$$\text{Tr}_{\hat{A}B_1B_2}\left[M_{A\hat{A}\hat{B}_1B_1\hat{B}_2B_2}\right] = I_{A\hat{B}_1\hat{B}_2}, \tag{178}$$

$$\left(\mathcal{F}_{\hat{B}_1\hat{B}_2}\otimes\mathcal{F}_{B_1B_2}\right)\left(M_{A\hat{A}\hat{B}_1B_1\hat{B}_2B_2}\right) = M_{A\hat{A}\hat{B}_1B_1\hat{B}_2B_2}, \tag{179}$$

$$\text{Tr}_{B_2}\left[M_{A\hat{A}\hat{B}_1B_1\hat{B}_2B_2}\right] = \frac{M_{A\hat{A}\hat{B}_1B_1}}{d_{\hat{B}}}\otimes I_{\hat{B}_2}, \tag{180}$$

$$T_{A\hat{A}}\left(M_{A\hat{A}\hat{B}_1B_1\hat{B}_2B_2}\right) \geqslant 0, \tag{181}$$

$$T_{\hat{B}_2B_2}\left(M_{A\hat{A}\hat{B}_1B_1\hat{B}_2B_2}\right) \geqslant 0, \tag{182}$$

$$\text{Tr}_{\hat{A}}\left[M_{A\hat{A}\hat{B}_1B_1\hat{B}_2B_2}\right] = I_A\otimes\frac{1}{d_A}\text{Tr}_{\hat{A}A}\left[M_{A\hat{A}\hat{B}_1B_1\hat{B}_2B_2}\right]. \tag{183}$$

The objective function and the first two constraints follow from the semidefinite program in (46) for the normalized diamond distance. The quantity

$$\text{Tr}_{\hat{A}\hat{B}_1}\left[T_{\hat{A}\hat{B}_1}\left(\Gamma^{\mathcal{N}}_{\hat{A}\hat{B}_1}\right) M_{A\hat{A}\hat{B}_1B_1}/d_{\hat{B}}\right] \tag{184}$$

in (177) is the Choi operator of the serial composition of the available channel $\mathcal{N}_{\hat{A}\to\hat{B}}$ and the superchannel with corresponding bipartite channel $\mathcal{K}_{A\hat{B}_1\to\hat{A}B_1}$, with Choi operator $M_{A\hat{A}\hat{B}_1B_1}/d_{\hat{B}}$, where $\mathcal{K}_{A\hat{B}_1\to\hat{A}B_1}$ is the marginal channel of $\mathcal{M}_{A\hat{B}_1\hat{B}_2\to\hat{A}B_1B_2}$, defined as

$$\mathcal{K}_{A\hat{B}_1\to\hat{A}B_1}\left(\omega_{A\hat{B}_1}\right) \coloneqq \text{Tr}_{B_2}\left[\mathcal{M}_{A\hat{B}_1\hat{B}_2\to\hat{A}B_1B_2}\left(\omega_{A\hat{B}_1}\otimes\pi_{\hat{B}_2}\right)\right]. \tag{185}$$

The constraint in (178) forces $\mathcal{M}_{A\hat{B}_1\hat{B}_2\to\hat{A}B_1B_2}$ to be trace preserving, that in (179) forces $\mathcal{M}_{A\hat{B}_1\hat{B}_2\to\hat{A}B_1B_2}$ to be permutation covariant with respect to the B systems [see (75)], and that in (180) forces $\mathcal{M}_{A\hat{B}_1\hat{B}_2\to\hat{A}B_1B_2}$ to be the extension of the marginal channel $\mathcal{K}_{A\hat{B}_1\to\hat{A}B_1}$. The final two PPT constraints are equivalent to the C-PPT-P constraints in (76) and (77), respectively.

B. SDP lower bound on the error of approximate quantum error correction

The semidefinite program in Proposition 8 can be simplified for the special case $\mathcal{N}_{A\to B} = \text{id}^d_{A\to B}$ by exploiting the unitary covariance symmetry of the identity channel, as stated in (65).

Proposition 9. The semidefinite program in Proposition 8, for the special case of simulating the identity channel $\text{id}^d_{A\to B}$, simplifies as follows for $d \geqslant 3$:

$$e_{\text{2PENS}}(\mathcal{N}_{\hat{A}\to\hat{B}}) = e^F_{\text{2PENS}}(\mathcal{N}_{\hat{A}\to\hat{B}}) \tag{186}$$

$$= 1 - \sup_{\substack{M^+,M^-,M^0\geqslant 0,\\ M^1,M^2,M^3\in\text{LinOp}}} \text{Tr}\left[T_{\hat{A}\hat{B}_1}\left(\Gamma^{\mathcal{N}}_{\hat{A}\hat{B}_1}\right)\frac{P_{\hat{A}\hat{B}_1\hat{B}_2}}{d_{\hat{B}}}\right], \tag{187}$$

subject to

$$\begin{bmatrix} M^0 + M^3 & M^1 - iM^2 \\ M^1 + iM^2 & M^0 - M^3 \end{bmatrix} \geqslant 0, \tag{188}$$

$$I_{\hat{B}_1\hat{B}_2} = \text{Tr}_{\hat{A}}\left[M^+_{\hat{A}\hat{B}_1\hat{B}_2} + M^-_{\hat{A}\hat{B}_1\hat{B}_2} + M^0_{\hat{A}\hat{B}_1\hat{B}_2}\right], \tag{189}$$

$$M^i_{\hat{A}\hat{B}_1\hat{B}_2} = \mathcal{F}_{\hat{B}_1\hat{B}_2}\left(M^i_{\hat{A}\hat{B}_1\hat{B}_2}\right) \quad \forall i\in\{+,-,0,1\}, \tag{190}$$

$$M^j_{\hat{A}\hat{B}_1\hat{B}_2} = -\mathcal{F}_{\hat{B}_1\hat{B}_2}\left(M^j_{\hat{A}\hat{B}_1\hat{B}_2}\right) \quad \forall j\in\{2,3\}, \tag{191}$$

$$P_{\hat{A}\hat{B}_1\hat{B}_2} = \frac{1}{d_{\hat{B}}}\text{Tr}_{\hat{B}_2}\left[P_{\hat{A}\hat{B}_1\hat{B}_2}\right]\otimes I_{\hat{B}_2}, \tag{192}$$

$$Q_{\hat{A}\hat{B}_1\hat{B}_2} = \frac{1}{d_{\hat{B}}}\text{Tr}_{\hat{B}_2}\left[Q_{\hat{A}\hat{B}_1\hat{B}_2}\right]\otimes I_{\hat{B}_2}, \tag{193}$$

$$P_{\hat{A}\hat{B}_1\hat{B}_2} \coloneqq \frac{1}{2d}[dM^0 + M^1 + \sqrt{d^2-1}\,M^2], \tag{194}$$

$$Q_{\hat{A}\hat{B}_1\hat{B}_2} \coloneqq \frac{1}{2d}\begin{bmatrix} 2d\left(M^+_{\hat{A}\hat{B}_1\hat{B}_2} + M^-_{\hat{A}\hat{B}_1\hat{B}_2}\right) + dM^0_{\hat{A}\hat{B}_1\hat{B}_2} \\ -M^1_{\hat{A}\hat{B}_1\hat{B}_2} - \sqrt{d^2-1}\,M^2_{\hat{A}\hat{B}_1\hat{B}_2} \end{bmatrix}, \tag{195}$$

$$T_{\hat{A}}\left(\frac{2M^+_{\hat{A}\hat{B}_1\hat{B}_2}}{d+2} + M^0_{\hat{A}\hat{B}_1\hat{B}_2} + M^1_{\hat{A}\hat{B}_1\hat{B}_2}\right) \geqslant 0, \tag{196}$$

$$T_{\hat{A}}\left(\frac{2M^-_{\hat{A}\hat{B}_1\hat{B}_2}}{d-2} + M^1_{\hat{A}\hat{B}_1\hat{B}_2} - M^0_{\hat{A}\hat{B}_1\hat{B}_2}\right) \geqslant 0, \tag{197}$$

$$\begin{bmatrix} G^0 + G^3 & G^1 - iG^2 \\ G^1 + iG^2 & G^0 - G^3 \end{bmatrix} \geqslant 0, \tag{198}$$

$$G^0_{\hat{A}\hat{B}_1\hat{B}_2} \coloneqq T_{\hat{A}}\left(M^+ + M^- + \frac{M^0 - dM^1}{2}\right), \tag{199}$$

$$G^1_{\hat{A}\hat{B}_1\hat{B}_2} \coloneqq T_{\hat{A}}\left(M^+ - M^- + \frac{M^1 - dM^0}{2}\right), \tag{200}$$

$$G^2_{\hat{A}\hat{B}_1\hat{B}_2} \coloneqq \frac{\sqrt{3(d^2-1)}}{2}T_{\hat{A}}\left(M^2_{\hat{A}\hat{B}_1\hat{B}_2}\right), \tag{201}$$

$$G^3_{\hat{A}\hat{B}_1\hat{B}_2} \coloneqq \frac{\sqrt{3(d^2-1)}}{2}T_{\hat{A}}\left(M^3_{\hat{A}\hat{B}_1\hat{B}_2}\right), \tag{202}$$

$$T_{\hat{A}\hat{B}_1}\left(\frac{dM^+}{d+2} + M^- + \frac{dM^0 - M^1 - \sqrt{d^2-1}\,M^2}{2}\right) \geqslant 0, \tag{203}$$

$$T_{\hat{A}\hat{B}_1}\left(M^+ + \frac{dM^-}{d-2} - \frac{dM^0 - M^1 - \sqrt{d^2-1}\,M^2}{2}\right) \geqslant 0, \tag{204}$$

$$\begin{bmatrix} E^0 + E^3 & E^1 - iE^2 \\ E^1 + iE^2 & E^0 - E^3 \end{bmatrix} \geqslant 0, \tag{205}$$

$$E^0_{\hat{A}\hat{B}_1\hat{B}_2} := \frac{T_{\hat{A}\hat{B}_1}\left(d(M^+ - M^-) + \frac{L^0}{2}\right)}{d^2-1}, \tag{206}$$

$$E^1_{\hat{A}\hat{B}_1\hat{B}_2} := \frac{T_{\hat{A}\hat{B}_1}\left(-M^+ + M^- + \frac{L^1}{2}\right)}{d^2-1}, \tag{207}$$

$$E^2_{\hat{A}\hat{B}_1\hat{B}_2} := \frac{T_{\hat{A}\hat{B}_1}\left(M^+ - M^- + \frac{L^2}{2}\right)}{\sqrt{d^2-1}}, \tag{208}$$

$$E^3_{\hat{A}\hat{B}_1\hat{B}_2} := T_{\hat{A}\hat{B}_1}\left(M^3_{\hat{A}\hat{B}_1\hat{B}_2}\right), \tag{209}$$

$$L^0 := (d^2-2)M^0 + dM^1 + d\sqrt{d^2-1}\,M^2, \tag{210}$$

$$L^1 := dM^0 + (2d^2-3)M^1 - \sqrt{d^2-1}\,M^2, \tag{211}$$

$$L^2 := M^1 - dM^0 - \sqrt{d^2-1}\,M^2, \tag{212}$$

$$\frac{\operatorname{Tr}_{\hat{A}}[2M^+]}{(d+2)(d-1)} = \frac{\operatorname{Tr}_{\hat{A}}[2M^+ + M^0 + M^1]}{d(d+1)}, \tag{213}$$

$$\frac{\operatorname{Tr}_{\hat{A}}[2M^-]}{(d-2)(d+1)} = \frac{\operatorname{Tr}_{\hat{A}}[2M^- + M^0 - M^1]}{d(d-1)}, \tag{214}$$

$$\frac{1}{2}\operatorname{Tr}_{\hat{A}}[M^0] = \frac{dI_{\hat{B}_1\hat{B}_2} + \operatorname{Tr}_{\hat{A}}[M^- - M^+ - M^1]}{d(d^2-1)}, \tag{215}$$

$$\frac{1}{2}\operatorname{Tr}_{\hat{A}}[M^1] = \frac{-I_{\hat{B}_1\hat{B}_2} + d\operatorname{Tr}_{\hat{A}}[M^+ - M^- + M^1]}{d(d^2-1)}, \tag{216}$$

$$\operatorname{Tr}_{\hat{A}}[M^2] = \operatorname{Tr}_{\hat{A}}[M^3] = 0. \tag{217}$$

For the case of $d = 2$, the SDP is the same, with the exception that we set $M^-_{\hat{A}\hat{B}_1\hat{B}_2} = 0$ and the constraints in (197), (204), and (214) are not used.

Proof. See Appendix E of the Supplemental Material [43]. ∎

We now provide expository remarks similar to Remarks 4 and 5, as well as an additional remark about approximate quantum error correction assisted by one-way LOCC.

Remark 10. The SDP in the statement of Proposition 9 is rather lengthy, and so we provide some explanation here. The constraint in (188) and the constraints $M^+, M^-, M^0 \geqslant 0$ in (187) correspond to the constraint of complete positivity in (175) (i.e., $M_{A\hat{A}\hat{B}_1B_1\hat{B}_2B_2} \geqslant 0$). The constraint in (189) corresponds to the constraint of trace preservation in (178). The constraints in (190)–(191) correspond to the constraint of permutation covariance in (179). The constraints in (192)–(193) correspond to the nonsignaling constraint in (180). The constraints in (196)–(198) correspond to the PPT constraint in (181), and the constraints in (203)–(205) correspond to the PPT constraint in (182). Finally, the constraints in (213)–(217) correspond to the nonsignaling constraint in (183).

Remark 11. Even though the number of constraints in the SDP above appears to increase when compared with the SDP from Proposition 8, we note that the runtime of the SDP above is significantly reduced because the size of the matrices involved in each of the constraints is much smaller. This is the main advantage that we get by incorporating unitary covariance symmetry of the identity channel.

If we only optimized over the larger set of 2-extendible channels instead of the set of 2-PPT-extendible nonsignaling channels, the SDP would be much simpler, given by (187)–(193). However, optimizing over the smaller set of 2-PPT-extendible nonsignaling channels gives tighter bounds at a marginal increase in computational cost, and thus we also include the PPT constraints in (196)–(198) and (203)–(205) and the nonsignaling constraints in (213)–(217).

Remark 12. By excluding the nonsignaling constraints in (213)–(217), the resulting SDP gives a lower bound on the simulation error of approximate quantum error correction assisted by a one-way LOCC channel. That is, the resulting SDP gives a lower bound on

$$e_{1\text{WL}}(\mathcal{N}_{\hat{A}\to\hat{B}}) := \inf_{\Lambda\in 1\text{WL}} e(\mathcal{N}_{\hat{A}\to\hat{B}}, \Lambda_{(\hat{A}\to\hat{B})\to(A\to B)}), \tag{218}$$

where

$$e_{1\text{WL}}(\mathcal{N}_{\hat{A}\to\hat{B}}, \Lambda_{(\hat{A}\to\hat{B})\to(A\to B)}) := \tfrac{1}{2}\left\| \mathrm{id}^d_{A\to B} - \Lambda_{(\hat{A}\to\hat{B})\to(A\to B)}(\mathcal{N}_{\hat{A}\to\hat{B}})\right\|_\diamond, \tag{219}$$

with Λ a one-way LOCC superchannel, as defined in (123). By the same reasoning given for Proposition 6, this error is no different if we use infidelity instead of normalized diamond distance.

VIII. EXAMPLES

In this section we present some numerical results from our semidefinite programs. To perform these numerical calculations, we employed CVXPY [50,51] with the interior point optimizer MOSEK. All of our Python source code is available with the arXiv posting of our paper.

A. Approximate teleportation and quantum error correction using special mixed states and channels

First, we provide bounds on the performance of approximate teleportation (i.e., on the error in simulating an identity channel), when using a particular set of imperfect resource states. In the past, PPT constraints alone (i.e., without 2-extendibility) have been used to obtain bounds on objective functions involving an optimization over the set of LOCC channels (see, e.g., [15,31–35]). We can also use them to obtain a lower bound on the simulation error of approximate teleportation. By following techniques similar to those in [15,31], we find the following SDP gives a lower bound on the simulation error of approximate teleportation:

$$1 - \sup_{K_{\hat{A}\hat{B}}\geqslant 0} \left\{ \begin{array}{c} \operatorname{Tr}[K_{\hat{A}\hat{B}}\rho_{\hat{A}\hat{B}}] : \\ K_{\hat{A}\hat{B}} \leqslant I_{\hat{A}\hat{B}}, \\ -I_{\hat{A}\hat{B}} \leqslant d\, T_{\hat{B}}(K_{\hat{A}\hat{B}}) \leqslant I_{\hat{A}\hat{B}} \end{array} \right\}. \tag{220}$$

See Appendix F of the Supplemental Material [43] for a proof. We note here that PPT constraints are implied by the 2-PPT-extendibility constraints given in Proposition 3, so that the optimal value in (220) is not smaller than the optimal value in (187). We also note that an SDP bearing some similarities to that in (220) was presented in [52], but that SDP calculates

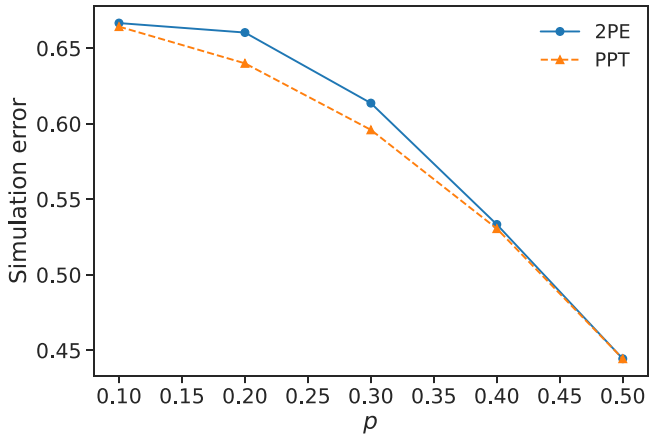

FIG. 1. Comparison between 2-PPT-extendiblity and PPT constraints for bounding the simulation error in approximate teleportation, when using the resource state $p\Phi_{\hat{A}\hat{B}} + (1-p)\pi_{\hat{A}} \otimes \sigma_{\hat{B}}$, where $p \in [0, 1]$. The plot shows that 2-PPT-extendibility gives slightly better bounds for $p < 0.5$. For higher values of p, the two curves become indistinguishable.

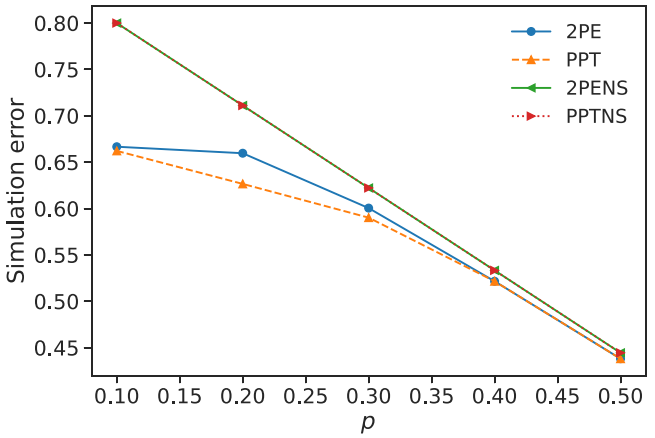

FIG. 2. Comparison between 2-PPT-extendiblity and PPT constraints for bounding the simulation error in approximate quantum error correction when using the resource channel with Choi state $p\Phi_{\hat{A}\hat{B}} + (1-p)\pi_{\hat{A}} \otimes \sigma_{\hat{B}}$, where $p \in [0, 1]$ and $\sigma_{\hat{B}}$ is defined in (222). PPTNS and 2PENS are the curves obtained using the SDPs in (223) and Proposition 9, respectively, giving lower bounds on the error in approximate quantum error correction. There is no significant difference in the numerical values obtained from these two conditions. PPT and 2PE are the curves obtained using the same SDPs but without the nonsignaling constraints, hence, giving lower bounds on the error in one-way LOCC-assisted approximate error correction.

a bound on one-shot distillable entanglement, whereas the SDP in (220) calculates a bound on the error of approximate teleportation.

In the following example, we show that 2-PPT-extendibility gives strictly stronger bounds than PPT constraints alone, when optimizing over one-way LOCC channels. Consider the following mixed state:

$$p\Phi_{\hat{A}\hat{B}} + (1-p)\pi_{\hat{A}} \otimes \sigma_{\hat{B}}, \tag{221}$$

where $p \in [0, 1]$, $\Phi_{\hat{A}\hat{B}}$ is the maximally entangled state of Schmidt rank three, $\pi_{\hat{A}}$ is the maximally mixed state of dimension three, and $\sigma_{\hat{B}}$ is a randomly selected 3×3 density matrix. Using the state in (221) as the resource for approximate teleportation, lower bounds on the simulation error, as given by 2-PPT-extendibility, are stronger than those given by PPT constraints alone, for small values of p. Figure 1 compares the lower bounds obtained for different values of p and randomly generated $\sigma_{\hat{B}}$. The state $\sigma_{\hat{B}}$ that was used to generate data for Fig. 1 is as follows:

$$\begin{bmatrix} 0.140 & 0.043+0.024i & -0.143+0.028i \\ 0.043-0.024i & 0.222 & -0.257+0.006i \\ -0.143-0.028i & -0.257-0.006i & 0.638 \end{bmatrix}. \tag{222}$$

We note here that the SDP calculations depend on the choice of $\sigma_{\hat{B}}$. For certain choices of $\sigma_{\hat{B}}$, the difference in the errors disappears for all values of p, e.g., when $\sigma_{\hat{B}}$ is a maximally mixed state. It still remains open to determine the full set of resource states for which 2-PPT-extendibility gives stronger bounds on the simulation error. Regardless, this example demonstrates that including 2-PPT-extendibility constraints can improve the bounds obtained using PPT constraints alone.

One can consider the same comparison for approximate quantum error correction. Using similar techniques, we derive the following SDP lower bound on the simulation error of approximate quantum error correction for a channel $\mathcal{N}_{\hat{A}\to\hat{B}}$, when using PPT and nonsignaling constraints only:

$$1 - \sup_{K_{\hat{A}\hat{B}}, \sigma_{\hat{A}} \geqslant 0} \left\{ \begin{array}{c} \operatorname{Tr}\left[K_{\hat{A}\hat{B}}\Gamma^{\mathcal{N}}_{\hat{A}\hat{B}}\right]: \\ K_{\hat{A}\hat{B}} \leqslant \sigma_{\hat{A}} \otimes I_{\hat{B}}, \\ d^2 \operatorname{Tr}_{\hat{A}}[K_{\hat{A}\hat{B}}] = I_{\hat{B}}, \\ \sigma_{\hat{A}} \otimes I_{\hat{B}} \pm d\, T_{\hat{B}}(K_{\hat{A}\hat{B}}) \geqslant 0, \\ \operatorname{Tr}[\sigma_{\hat{A}}] = 1. \end{array} \right\}. \tag{223}$$

See Appendix G of the Supplemental Material [43] for a proof. We note here that essentially the same SDP was given in [31] (up to a transpose in the objective function). The SDP in [31] resulted from taking the error criterion to be in terms of entanglement fidelity when transmitting the maximally entangled state. Our proof here clarifies that essentially the same SDP results when using normalized diamond distance or channel infidelity as the error criterion. The second constraint in the SDP ($d^2 \operatorname{Tr}_{\hat{A}}[K_{\hat{A}\hat{B}}] = I_{\hat{B}}$) corresponds to the nonsignaling condition. Following the same reasoning as in Remark 10, removing this constraint leads to an SDP that provides a lower bound on the simulation error of approximate quantum error correction assisted by one-way LOCC.

The example state in (221) can also serve as the Choi state of a channel, due to the fact that the reduced state of system $\hat{A}$ is maximally mixed. In Fig. 2 we plot the lower bound in (223) and the lower bound from Proposition 9 for the corresponding channel. Additionally, we also plot the simulation errors that result from excluding the nonsignaling constraints from both SDPs. The resulting SDPs provide lower bounds on the errors in approximate quantum error correction assisted by one-way LOCC using PPT and 2-PPT-extendibility, respectively. Figure 2 demonstrates that the lower bound in Proposition 9 improves upon (223) for one-way LOCC simulation but provides no advantage for LOCR simulation. The

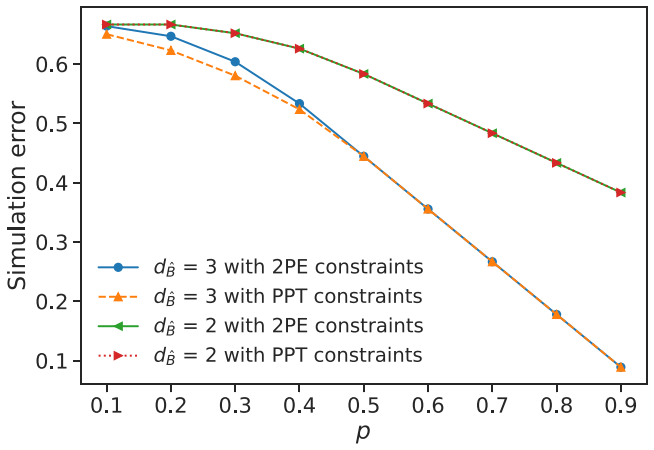

FIG. 3. Comparison between bounds on the simulation error for approximate teleportation when using a two-dimensional special mixed state and a three-dimensional special mixed state as a resource to teleport a two dimensional state. The resource state is of the form $p\Phi_{\hat{A}\hat{B}} + (1-p)\pi_{\hat{A}} \otimes \sigma_{\hat{B}}$, where $p \in [0, 1]$ and $\sigma_{\hat{B}}$ is chosen to be (225) when $d_{\hat{B}} = 2$ and (226) when $d_{\hat{B}} = 3$. The bounds on the simulation error are calculated using both the 2PE constraints given in Proposition 3 and the PPT constraints given in (220). There is no significant difference in the numerical values obtained from both constraints for $d_{\hat{B}} = 2$.

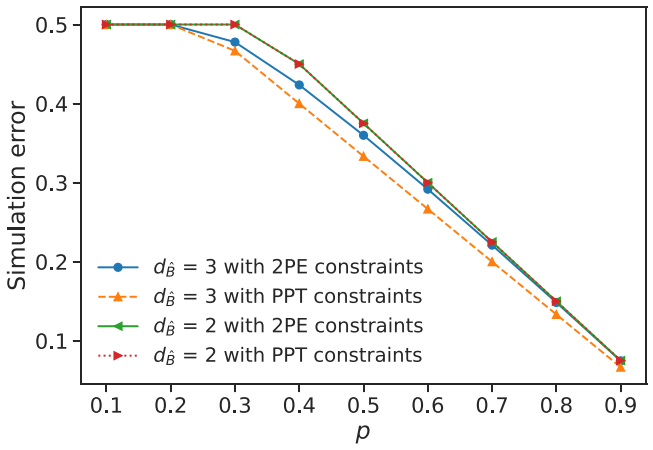

FIG. 4. Lower bounds on the simulation error of approximate quantum error correction for depolarizing channels when simulating a two-dimensional identity channel. The bounds are calculated using the SDP in Proposition 9 with 2-PPT-extendibility constraints, and the SDP in (223) with PPT constraints only, for different dimensions of the depolarizing channel ($d_{\hat{B}} = 2$ and $d_{\hat{B}} = 3$). There is no significant difference in the numerical values obtained from PPT and 2-PPT-extendibility constraints for $d_{\hat{B}} = 2$. The bounds are obtained without the nonsignaling constraints, hence, corresponding to one-way LOCC simulation.

difference between all four curves becomes very small (less than 10^{-3}) for higher values of p.

B. Three-dimensional approximate teleportation using two-dimensional special mixed states

In this example, we investigate the simulation error in approximate teleportation when a lower dimensional imperfect resource state is used to teleport a higher dimensional state. We use a similar resource state as in (221):

$$\rho_{\hat{A}\hat{B}} = p\Phi_{\hat{A}\hat{B}} + (1-p)\pi_{\hat{A}} \otimes \sigma'_{\hat{B}}, \tag{224}$$

but the maximally entangled and maximally mixed states are two-dimensional. Additionally, $\sigma'_{\hat{B}}$ was generated randomly and is taken as

$$\sigma'_{\hat{B}} = \begin{bmatrix} 0.287 & -0.347 + 0.132i \\ -0.347 - 0.132i & 0.713 \end{bmatrix}. \tag{225}$$

In Fig. 3 we plot the bounds on the simulation error versus the parameter p in (224), when using the 2PE constraints given in Proposition 3 and the PPT constraints given in (220). We also compare this to the bounds on the simulation error when using a three-dimensional special mixed state instead. The resource state used is the same as the state in (221), but $\sigma_{\hat{B}}$ is chosen as follows:

$$\begin{bmatrix} 0.287 & -0.347 + 0.132i & 0 \\ -0.347 - 0.132i & 0.713 & 0 \\ 0 & 0 & 0 \end{bmatrix}, \tag{226}$$

in order to provide a closer comparison with the two-dimensional case in (224).

We see from Fig. 3 that a two-dimensional resource state with a small amount of imperfection can outperform a three-dimensional resource with higher amounts of imperfection for the task of three-dimensional approximate teleportation. We also notice that the 2PE constraints and the PPT constraints give the same error values when $d_{\hat{B}} = 2$, but give different values when $d_{\hat{B}} = 3$, as seen in Fig. 1 as well.

C. Approximate quantum error correction for depolarizing channels

In this example, we investigate the simulation error in approximate error correction for qubit and qutrit depolarizing channels, with the goal of simulating a qubit identity channel. The Choi state of the depolarizing channel $\mathcal{D}_{\hat{A}\to\hat{B}}$ is given by

$$\Phi^{\mathcal{D}}_{\hat{A}\hat{B}} := p\Phi_{\hat{A}\hat{B}} + (1-p)\pi_{\hat{A}\hat{B}}, \tag{227}$$

where $p \in [0, 1]$, $\Phi_{\hat{A}\hat{B}}$ is the maximally entangled state, and $\pi_{\hat{A}\hat{B}}$ is the maximally mixed state. For a qubit depolarizing channel, $d_{\hat{A}} = d_{\hat{B}} = 2$, and for a qutrit depolarizing channel, $d_{\hat{A}} = d_{\hat{B}} = 2$.

In Fig. 4 we plot the lower bounds on the simulation error of approximate error correction for a depolarizing channel, when simulating a qubit identity channel. The bounds are obtained using the 2-PPT-extendibility conditions from Proposition 9 and using the PPT conditions from (223). The bounds are calculated for the case of one-way LOCC assistance, i.e., by ignoring the nonsignaling constraints in (213)–(217) and the constraint $d^2 \operatorname{Tr}_{\hat{A}}[K_{\hat{A}\hat{B}}] = I_{\hat{B}}$ in (223), respectively. We notice from Fig. 4 that the 2-PPT-extendibility constraints give better bounds compared to the PPT constraints when using a three-dimensional depolarizing channel to simulate a two-dimensional identity channel. However, both sets of constraints give the same bounds when a two-dimensional depolarizing channel is used to simulate a two-dimensional identity channel. This was also observed in the numerical calculations of [18].

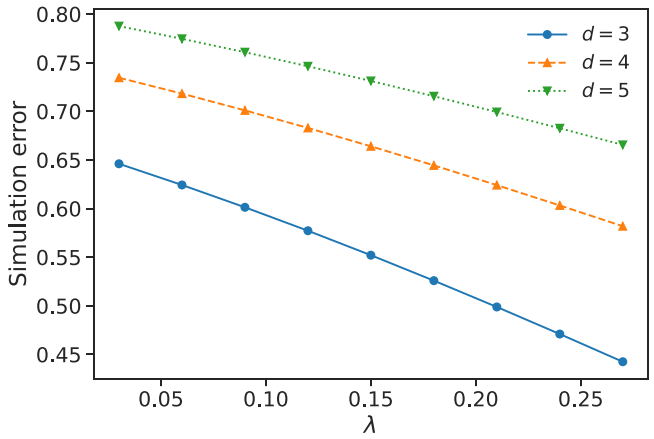

FIG. 5. Lower bounds on the simulation error of unideal teleportation when using the two-mode squeezed vacuum state as the resource state. The parameter $\lambda = \tanh(r)$, where r is the squeezing parameter. Larger values of λ correspond to larger values of entanglement, which leads to a smaller error in simulating the identity channel.

We also note that a three-dimensional depolarizing channel provides little advantage over a two-dimensional depolarizing channel for simulating a two-dimensional identity channel. Therefore, a two-dimensional depolarizing channel with a slightly higher value of the parameter p can outperform a three-dimensional depolarizing channel with a lower value of p, for the purpose of approximating a qubit identity channel.

D. Approximate teleportation using the two-mode squeezed vacuum state

Two-mode squeezed vacuum states are easily prepared in laboratories and have entanglement content that can be parameterized by $\lambda \geqslant 0$. They are defined as [53]

$$\sqrt{1-\lambda^2}\sum_{n=0}^{\infty}\lambda^n|n\rangle|n\rangle. \tag{228}$$

They are used as a resource state in continuous-variable quantum teleportation [54] and have also been used as a resource in experiments on teleportation of photonic qubits [4,55]. Here we investigate bounds on the performance of qudit teleportation with the two-mode squeezed vacuum state as the resource state.

The parameter λ denotes the strength of squeezing applied ($\lambda = \tanh(r)$, where r is the squeezing parameter). For low squeezing strength, we can ignore higher order terms in λ without inducing much error. We use the following state in our calculations for qudit teleportation:

$$\frac{1}{\sqrt{1+\lambda^2+\lambda^4}}\sum_{n=0}^{2}\lambda^n|n\rangle|n\rangle. \tag{229}$$

However, for higher values of the squeezing strength (i.e., λ near to one), we do not expect this approximation to be good.

Figure 5 demonstrates that the simulation error increases with d for fixed values of λ, where d is the dimension of the target identity channel that the protocol is simulating. The simulation error does not go to zero for $d > 3$, even for maximally entangled qutrit resource states. Therefore, projecting this trend further, we conclude that simulation of a higher-dimensional identity channel with a lower-dimensional resource state incurs larger errors in the simulation. We note here that we observed no difference in the values calculated by the SDPs in (223) and Proposition 9.

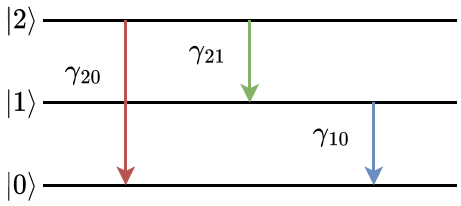

FIG. 6. Action of an amplitude damping channel on a three-level quantum system. The parameters γ_{10}, γ_{20}, and γ_{21} represent decay rates between the respective levels.

E. Approximate quantum error correction for a three-level amplitude damping channel

Here we present an example of our bound for the simulation error in approximate error correction. We consider a three-level amplitude damping channel, as defined in [22], to demonstrate our SDP in Proposition 9.

The channel can be defined using three decay parameters, labeled by the states involved: $(\gamma_{10}, \gamma_{21}, \gamma_{20})$. See Fig. 6 for a depiction. The Kraus operators for the three-level amplitude damping channel are as follows:

$$K_0 := \begin{bmatrix} 1 & 0 & 0 \\ 0 & \sqrt{1-\gamma_{10}} & 0 \\ 0 & 0 & \sqrt{1-\gamma_{21}-\gamma_{20}} \end{bmatrix}, \tag{230}$$

$$K_1 := \begin{bmatrix} 0 & \sqrt{\gamma_{10}} & 0 \\ 0 & 0 & 0 \\ 0 & 0 & 0 \end{bmatrix}, \tag{231}$$

$$K_2 := \begin{bmatrix} 0 & 0 & 0 \\ 0 & 0 & \sqrt{\gamma_{21}} \\ 0 & 0 & 0 \end{bmatrix}, \tag{232}$$

$$K_3 := \begin{bmatrix} 0 & 0 & \sqrt{\gamma_{20}} \\ 0 & 0 & 0 \\ 0 & 0 & 0 \end{bmatrix}, \tag{233}$$

so that its action on an input state ρ is given by $\sum_{i=0}^{3} K_i \rho K_i^\dagger$. For the map to be completely positive and trace preserving, the decay parameters must obey

$$\begin{cases} 0 \leqslant \gamma_i \leqslant 1 & \forall i \in \{10, 21, 20\} \\ \gamma_{21} + \gamma_{20} \leqslant 1 \end{cases}. \tag{234}$$

Figure 7 plots the lower bound on the simulation error as a function of the decay parameter γ_{10}, for various values of the other decay parameters. We notice in Fig. 7 that the simulation error monotonically increases with the decay parameters. As all three decay parameters approach zero, the channel becomes close to an identity channel. This is reflected in the plot as the simulation error also approaches zero. We note here

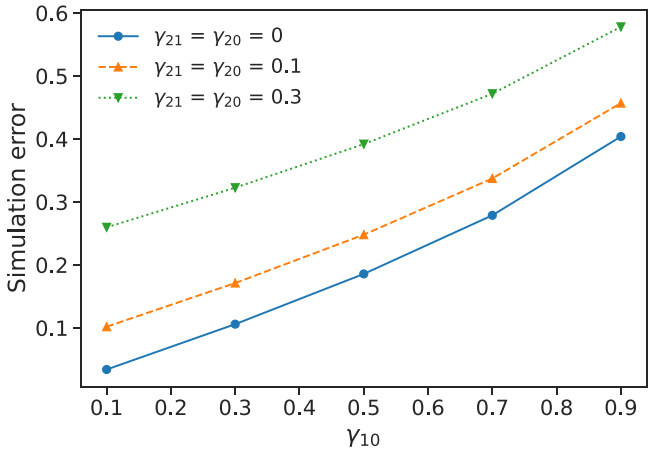

FIG. 7. Lower bounds on the simulation error of approximate quantum error correction when using a three-level amplitude damping channel. The parameters γ_{10}, γ_{21}, and γ_{20} are decay parameters for the labeled states. The dimension d of the target identity channel is set equal to the input and output dimensions (equal to three) of the amplitude-damping channel.

that we observed no difference in the values calculated by the SDPs in (223) and Proposition 9.

F. Comparison of computational runtimes

In this section we present the average runtime to execute various SDPs listed in this work. The calculations were performed on a computer with 16 GB RAM and an Intel i7-9750H processor.

All calculations that generated the entries in Table I employed the two-dimensional maximally entangled state. For approximate teleportation, the input is the maximally entangled state of Schmidt rank two, and for approximate error correction, the input is the qubit identity channel. The simulated channel is also the qubit identity channel in all cases. The runtimes were calculated using time.time() function in Python. They are only presented for the purpose of comparison and can vary moderately.

All runtimes are listed in Table I, where we see that the unsimplified SDP for approximate teleportation with 2-PPT-extendibility, given in Proposition 2, is around 25 times slower than the simplified SDP for the same in Proposition 3. The SDP for the simulation error in approximate teleportation using PPT constraints that is given in (220) is several times faster than when 2-PPT-extendibility constraints are employed, but we have seen in the examples that 2-PPT-extendibility constraints can give tighter lower bounds on the simulation error.

TABLE I. Comparing the runtime of different SDPs presented in this work. 2PE refers to 2-PPT-extendibility constraints and NS indicates that nonsignaling conditions were used. All calculations were done for a two-dimensional resource state and simulating the two-dimensional identity channel.

SDP	Runtime (s)
Teleportation unsimplified 2PE	253.03
Teleportation 2PE	10.34
Teleportation PPT	0.19
Error correction unsimplified	147.75
Error correction unsimplified 2PENS	158.22
Error correction 2PENS	5.65
Error correction 2PE	5.38
Error correction PPTNS	0.20
Error correction PPT	0.16

Similarly, we see that the unsimplified SDP for approximate error correction when using 2-PPT-extendibility constraints (Proposition 8) is several times slower than the simplified SDP given in Proposition 9. Again, the SDP with PPT constraints given in (223) is much faster than the SDP with 2-PPT-extendibility constraints, but we have demonstrated examples for which 2-PPT-extendibility constraints provide a tighter lower bound on the simulation error.

IX. CONCLUSION

In this work, we developed a technique for quantifying the performance of approximate teleportation using an arbitrary resource state, by establishing a lower bound on the error in simulating a teleportation protocol that uses an imperfect resource state and one-way LOCC channels. We accomplished this by combining the notions of C-PPT-P channels and 2-extendible channels to give a relaxation of the set of one-way LOCC channels, as was done previously in [18] but for approximate quantum error correction. We significantly reduced the complexity of our semidefinite program by exploiting the unitary covariance symmetry of the simulated identity channel. This symmetry is useful in semidefinite programs and can have much wider applications with respect to dynamical resource theories. As an example, we evaluated our lower bound when using a two-mode squeezed vacuum state as the resource state for approximate teleportation.

We used related techniques to quantify the performance of approximate quantum error correction. Incorporating 2-PPT-extendibility constraints again led to computationally feasible semidefinite optimizations for evaluating lower bounds on the error in approximate quantum error correction. We further exploited the unitary covariance symmetry of the identity channel to give a less computationally taxing semidefinite program to calculate the error. Finally, we demonstrated some calculations for amplitude damping channels as the resource channels.

The SDPs in this work provide computational support to ongoing experimental research in quantum information by providing tools to analyze available resources and identify valuable states and channels.

Several directions for future work remain open:

(1) We have only considered 2-extendible channels; incorporation of k-extendible channels for $k > 2$ into our semidefinite optimization could offer tighter bounds on the measures we have described. The recent work of [56] might be helpful for addressing this problem. The notion of 2-PPT-extendible channels is interesting in its own right via its connection with one-way LOCC channels.

(2) It would also be interesting to find semidefinite constraints on one-way LOCC and LOCR channels, beyond those presented here, which include k-extendibility, PPT, and nonsignaling.

(3) One could also try to find semidefinite tightenings of one-way LOCC and LOCR, which would lead to upper bounds on the simulation errors.

(4) The paper [15] shows that PPT constraints are sufficient to determine the exact simulation error in bidirectional teleportation for certain special states. Future work can identify a class of resource states that saturate the error bound using 2-PPT-extendibility constraints, e.g., states that are PPT but 2-unextendible. Such a class of states can offer insight not only in the study of teleportation protocols, but also to entanglement of states and channels.

ACKNOWLEDGMENTS

We thank Mario Berta, Eric Chitambar, Arshag Danageozian, Felix Leditzky, and Aliza Siddiqui for helpful discussions. This material is based upon work supported by the National Science Foundation under Award No. OAC-1852454 with additional support from the Center for Computation & Technology at Louisiana State University. V.S. and M.M.W. acknowledge support from the National Science Foundation under Grant No. 1907615.

APPENDIX: PROOF OF EQ. (12)

We provide a proof of (12) here. Consider that

$$\begin{aligned}
&\mathrm{Tr}_{B_1'} \circ \mathcal{N}_{AB_1\to A'B_1'} \\
&\quad = \mathrm{Tr}_{B_1'B_2} \circ \left(\mathcal{N}_{AB_1\to A'B_1'} \otimes \mathcal{P}^{\pi}_{B_2}\right) && \text{(A1)}\\
&\quad = \mathrm{Tr}_{B_1'B_2'} \circ \mathcal{M}_{AB_1B_2\to A'B_1'B_2'} \circ \mathcal{P}^{\pi}_{B_2} && \text{(A2)}\\
&\quad = \mathrm{Tr}_{B_1'B_2'} \circ \mathcal{F}_{B_1'B_2'} \circ \mathcal{M}_{AB_1B_2\to A'B_1'B_2'} \circ \mathcal{F}_{B_1B_2} \circ \mathcal{P}^{\pi}_{B_2} && \text{(A3)}\\
&\quad = \mathrm{Tr}_{B_1'B_2'} \circ \mathcal{M}_{AB_1B_2\to A'B_1'B_2'} \circ \mathcal{P}^{\pi}_{B_1} \circ \mathrm{id}_{B_1\to B_2} && \text{(A4)}\\
&\quad = \mathrm{Tr}_{B_1'} \circ \mathcal{N}_{AB_1\to A'B_1'} \circ \mathcal{P}^{\pi}_{B_1} \circ \mathrm{Tr}_{B_2} \circ \mathrm{id}_{B_1\to B_2} && \text{(A5)}\\
&\quad = \mathrm{Tr}_{B_1'} \circ \mathcal{N}_{AB_1\to A'B_1'} \circ \mathcal{R}^{\pi}_{B_1}. && \text{(A6)}
\end{aligned}$$

The first equality follows because $\mathcal{P}^{\pi}_{B_2}$ is a preparation channel that prepares the maximally mixed state π_{B_2} on system B_2, and then we trace it out. The second equality follows by using the nonsignaling property in (11). The third equality follows from permutation covariance of the channel $\mathcal{M}_{AB_1B_2\to A'B_1'B_2'}$ [i.e., the assumption that (10) holds]. The fourth equality follows because $\mathcal{F}_{B_1'B_2'}$ is a unitary channel, so that

$$\mathrm{Tr}_{B_1'B_2'} \circ \mathcal{F}_{B_1'B_2'} = \mathrm{Tr}_{B_1'B_2'}. \tag{A7}$$

Additionally, we used the fact that

$$\mathcal{F}_{B_1B_2} \circ \mathcal{P}^{\pi}_{B_2} = \mathcal{P}^{\pi}_{B_1} \circ \mathrm{id}_{B_1\to B_2}, \tag{A8}$$

where $\mathrm{id}_{B_1\to B_2}$ is an identity channel that transforms system B_1 to B_2. The fifth equality again invokes the nonsignaling property in (11). The last equality follows because

$$\mathcal{P}^{\pi}_{B_1} \circ \mathrm{Tr}_{B_2} \circ \mathrm{id}_{B_1\to B_2} = \mathcal{R}^{\pi}_{B_1}. \tag{A9}$$

That is, $\mathrm{Tr}_{B_2} \circ \mathrm{id}_{B_1\to B_2}$ is equivalent to Tr_{B_1}, so that this action combined with $\mathcal{P}^{\pi}_{B_1}$ realizes a replacer channel.

[1] C. H. Bennett, G. Brassard, C. Crépeau, R. Jozsa, A. Peres, and W. K. Wootters, Teleporting an unknown quantum state via dual classical and Einstein-Podolsky-Rosen channels, Phys. Rev. Lett. **70**, 1895 (1993).

[2] C. H. Bennett, D. P. DiVincenzo, J. A. Smolin, and W. K. Wootters, Mixed-state entanglement and quantum error correction, Phys. Rev. A **54**, 3824 (1996).

[3] D. Bouwmeester, J.-W. Pan, K. Mattle, M. Eibl, H. Weinfurter, and A. Zeilinger, Experimental quantum teleportation, Nature (London) **390**, 575 (1997).

[4] A. Furusawa, J. L. Sørensen, S. L. Braunstein, C. A. Fuchs, H. J. Kimble, and E. S. Polzik, Unconditional quantum teleportation, Science **282**, 706 (1998).

[5] D. Boschi, S. Branca, F. De Martini, L. Hardy, and S. Popescu, Experimental Realization of Teleporting an Unknown Pure Quantum State via Dual Classical and Einstein-Podolsky-Rosen Channels, Phys. Rev. Lett. **80**, 1121 (1998).

[6] M. Riebe, H. Häffner, C. F. Roos, W. Hänsel, J. Benhelm, G. P. T. Lancaster, T. W. Körber, C. Becher, F. Schmidt-Kaler, D. F. V. James, and R. Blatt, Deterministic quantum teleportation with atoms, Nature (London) **429**, 734 (2004).

[7] R. Ursin, T. Jennewein, M. Aspelmeyer, R. Kaltenbaek, M. Lindenthal, P. Walther, and A. Zeilinger, Quantum teleportation across the Danube, Nature (London) **430**, 849 (2004).

[8] J. F. Sherson, H. Krauter, R. K. Olsson, B. Julsgaard, K. Hammerer, I. Cirac, and E. S. Polzik, Quantum teleportation between light and matter, Nature (London) **443**, 557 (2006).

[9] X.-S. Ma, T. Herbst, T. Scheidl, D. Wang, S. Kropatschek, W. Naylor, B. Wittmann, A. Mech, J. Kofler, E. Anisimova *et al.*, Quantum teleportation over 143 kilometres using active feed-forward, Nature (London) **489**, 269 (2012).

[10] J.-G. Ren, P. Xu, H.-L. Yong, L. Zhang, S.-K. Liao, J. Yin, W.-Y. Liu, W.-Q. Cai, M. Yang, L. Li *et al.*, Ground-to-satellite quantum teleportation, Nature (London) **549**, 70 (2017).

[11] S. Popescu, Bell's inequalities versus teleportation: What Is Nonlocality?, Phys. Rev. Lett. **72**, 797 (1994).

[12] M. Horodecki, P. Horodecki, and R. Horodecki, General teleportation channel, singlet fraction, and quasidistillation, Phys. Rev. A **60**, 1888 (1999).

[13] C. H. Bennett, G. Brassard, S. Popescu, B. Schumacher, J. A. Smolin, and W. K. Wootters, Purification of Noisy Entanglement and Faithful Teleportation via Noisy Channels, Phys. Rev. Lett. **76**, 722 (1996).

[14] E. Kaur and M. M. Wilde, Amortized entanglement of a quantum channel and approximately teleportation-simulable channels, J. Phys. A: Math. Theor. **51**, 035303 (2018).

[15] A. U. Siddiqui and M. M. Wilde, Quantifying the performance of bidirectional quantum teleportation, arXiv:2010.07905v2.

[16] E. Kaur, S. Das, M. M. Wilde, and A. Winter, Extendibility Limits the Performance of Quantum Processors, Phys. Rev. Lett. **123**, 070502 (2019).

[17] E. Kaur, S. Das, M. M. Wilde, and A. Winter, Resource theory of unextendibility and nonasymptotic quantum capacity, Phys. Rev. A **104**, 022401 (2021).

[18] M. Berta, F. Borderi, O. Fawzi, and V. Scholz, Semidefinite programming hierarchies for constrained bilinear optimization, Math. Program. **194**, 781 (2022).
[19] A. Kitaev, Quantum computations: Algorithms and error correction, Russ. Math. Surv. **52**, 1191 (1997).
[20] A. Gilchrist, N. K. Langford, and M. A. Nielsen, Distance measures to compare real and ideal quantum processes, Phys. Rev. A **71**, 062310 (2005).
[21] G. Chiribella, G. M. D'Ariano, and P. Perinotti, Transforming quantum operations: Quantum supermaps, Europhys. Lett. **83**, 30004 (2008).
[22] S. Chessa and V. Giovannetti, Quantum capacity analysis of multi-level amplitude damping channels, Commun. Phys. **4**, 22 (2021).
[23] M. Hayashi, *Quantum Information Theory: Mathematical Foundation*, 2nd ed. (Springer, Berlin, 2017).
[24] A. S. Holevo, *Quantum Systems, Channels, Information: A Mathematical Introduction*, 2nd ed. (Walter de Gruyter, 2019).
[25] J. Watrous, *The Theory of Quantum Information* (Cambridge University Press, 2018).
[26] M. M. Wilde, *Quantum Information Theory*, 2nd ed. (Cambridge University Press, 2017).
[27] S. Khatri and M. M. Wilde, Principles of quantum communication theory: A modern approach, arXiv:2011.04672v1.
[28] E. M. Rains, Bound on distillable entanglement, Phys. Rev. A **60**, 179 (1999).
[29] E. M. Rains, A semidefinite program for distillable entanglement, IEEE Trans. Inf. Theory **47**, 2921 (2001).
[30] E. Chitambar, J. I. de Vicente, M. W. Girard, and G. Gour, Entanglement manipulation beyond local operations and classical communication, J. Math. Phys. **61**, 042201 (2020).
[31] D. Leung and W. Matthews, On the power of PPT-preserving and non-signalling codes, IEEE Trans. Inf. Theory **61**, 4486 (2015).
[32] X. Wang, W. Xie, and R. Duan, Semidefinite programming strong converse bounds for classical capacity, IEEE Trans. Inf. Theory **64**, 640 (2018).
[33] X. Wang and R. Duan, A semidefinite programming upper bound of quantum capacity, in *2016 IEEE International Symposium on Information Theory (ISIT)* (IEEE, 2016), pp. 1690–1694.
[34] X. Wang and R. Duan, An improved semidefinite programming upper bound on distillable entanglement, Phys. Rev. A **94**, 050301(R) (2016).
[35] M. Berta and M. M. Wilde, Amortization does not enhance the max-Rains information of a quantum channel, New J. Phys. **20**, 053044 (2018).
[36] A. C. Doherty, P. A. Parrilo, and F. M. Spedalieri, Distinguishing Separable and Entangled States, Phys. Rev. Lett. **88**, 187904 (2002).
[37] A. C. Doherty, P. A. Parrilo, and F. M. Spedalieri, Complete family of separability criteria, Phys. Rev. A **69**, 022308 (2004).
[38] J. Watrous, Semidefinite programs for completely bounded norms, Theory Comput. **5**, 217 (2009).
[39] A. Uhlmann, The "transition probability" in the state space of a *-algebra, Rep. Math. Phys. **9**, 273 (1976).
[40] H. Yuan and C.-H. F. Fung, Fidelity and Fisher information on quantum channels, New J. Phys. **19**, 113039 (2017).
[41] V. Katariya and M. M. Wilde, Geometric distinguishability measures limit quantum channel estimation and discrimination, Quant. Inf. Proc. **20**, 78 (2021).
[42] K. Fang, X. Wang, M. Tomamichel, and M. Berta, Quantum channel simulation and the channel's smooth max-information, IEEE Trans. Inf. Theory **66**, 2129 (2020).
[43] See Supplemental Material at http://link.aps.org/supplemental/10.1103/PhysRevA.107.012428 for detailed mathematical proofs of several propositions and equations in the main paper.
[44] L. Gurvits, Classical complexity and quantum entanglement, J. Comput. Syst. Sci. **69**, 448 (2004).
[45] S. Gharibian, Strong NP-hardness of the quantum separability problem, Quantum Inf. Comput. **10**, 343 (2010).
[46] G. Chiribella, G. M. D'Ariano, and P. Perinotti, Theoretical framework for quantum networks, Phys. Rev. A **80**, 022339 (2009).
[47] G. Chiribella, G. M. D'Ariano, and P. Perinotti, Memory Effects in Quantum Channel Discrimination, Phys. Rev. Lett. **101**, 180501 (2008).
[48] G. Gour, Comparison of quantum channels with superchannels, IEEE Trans. Inf. Theory **65**, 5880 (2019).
[49] B. Schumacher and M. D. Westmoreland, Approximate quantum error correction, Quant. Inf. Proc. **1**, 5 (2002).
[50] S. Diamond and S. Boyd, CVXPY: A Python-embedded modeling language for convex optimization, J. Machine Learn. Res. **17**, 1 (2016).
[51] A. Agrawal, R. Verschueren, S. Diamond, and S. Boyd, A rewriting system for convex optimization problems, J. Control Decision **5**, 42 (2018).
[52] K. Fang, X. Wang, M. Tomamichel, and R. Duan, Non-asymptotic entanglement distillation, IEEE Trans. Inf. Theory **65**, 6454 (2019).
[53] A. Serafini, *Quantum Continuous Variables: A Primer of Theoretical Methods* (CRC Press, 2017).
[54] S. L. Braunstein and H. J. Kimble, Teleportation of Continuous Quantum Variables, Phys. Rev. Lett. **80**, 869 (1998).
[55] S. Takeda, T. Mizuta, M. Fuwa, P. V. Loock, and A. Furusawa, Deterministic quantum teleportation of photonic quantum bits by a hybrid technique, Nature (London) **500**, 315 (2013).
[56] D. Grinko and M. Ozols, Linear programming with unitary-equivariant constraints, arXiv:2207.05713.